# Comparative Transcriptomics of Naturally Susceptible and Resistant *Trypanosoma cruzi* Strains in Response to Benznidazole

**Carlos Mario Ospina Varon**

**Universidad del Rosario**

**Facultad de Ciencias Naturales**

**Bogotá, Colombia**

**2025**

# Comparative Transcriptomics of Naturally Susceptible and Resistant *Trypanosoma cruzi* Strains in Response to Benznidazole

**Carlos Mario Ospina Varón**

Tesis presentada como requisito para la obtención del título de:

**Magister en Ciencias Naturales**

Director

Juan David Ramírez, PhD.

Profesor Titular

Facultad de Ciencias Naturales

Universidad del Rosario

**Facultad de Ciencias Naturales**

**Maestría en Ciencias Naturales**

**Universidad del Rosario**

**Bogotá, Colombia**

**2025**

**ACKNOWLEDGMENTS**

*Mi más sincero agradecimiento a la Universidad del Rosario, a la Facultad de Ciencias Naturales, a la Fundación Cardio Infantil, y al Ministerio de Ciencia, Tecnología e Innovación (CT 749-2021) por brindarme el apoyo, espacio y financiamiento necesario para culminar con éxito este proyecto.*

*A mi director Juan David Ramírez y a las directoras técnicas de GIMUR, Luz Helena y Marina Muñoz, les agradezco profundamente por ser una fuente de inspiración, apoyo y guía durante el proceso de mi maestría. Les agradezco profundamente porque me enseñaron que en el camino de la ciencia si existen excelentes investigadores, que a su vez son excelentes personas.*

*A mis padres Mario y Cecilia, y a mi hermano Juancho por darme su apoyo, amor y comprensión, y siempre estar ahí cuando más los necesito.*

*A Leidy por haber estado conmigo desde el principio de este proceso, por haber sido mi compañera de aventuras, por haberme enseñado muchas cosas a nivel personal y por haber compartido conmigo tantas experiencias inolvidables. De corazón le deseo hoy y siempre lo mejor en su vida.*

*A Tatiana por ser mi compinche de experimentos, por haberme enseñado el valor de una amistad sincera, por regañarme y ponerme los pies en la tierra cuando más lo necesitaba.*

*A Angie y Vanessa por escucharme, hacerme reír y siempre estar dispuestas a tener una charla cuando la ocasión la amerita.*

*A Lissa Cruz por brindarme la oportunidad de conocer a GIMUR, por darme las herramientas y enseñarme un montón de cosas en el laboratorio. Por ser una excelente tutora y una gran amiga.*

*A Stivenn por ayudarme en la parte experimental de mi trabajo de grado y haber sido mi compañero de materias y chisme durante mi estancia en el grupo.*

*En general a todos los miembros de GIMUR, porque siempre están dispuestos a ayudar y por haber sido mi segunda familia.*

*A mis amigos de Ibagué, Julián Barbosa, Brayhan Suarez, Ramiro, Juan Borja, Laura Devia, Camila Escobar, Rafa y Kata por escucharme y ser un apoyo emocional.*

*A mis amigos Cristian y Weimar por traer un poquito de la calidez de Ibagué y estar conmigo en las buenas y malas.*

*A mis amigos no académicos Julian R (Chiki), Alejandro (Nano) y Camilo (Milo) por sacarme miles de alegrías en momentos que ellos no sabían que los necesitaba.*

*Finalmente quiero agradecerme a mí por no desistir cuando las cosas se pusieron bastante oscuras y dar lo mejor de mí, aunque me estuviera quebrando por dentro.*

**Comparative Transcriptomics of Naturally Susceptible and Resistant *Trypanosoma cruzi* Strains in Response to Benznidazole**

Carlos Ospina[1], Tatiana Cáceres[1], Stivenn Gutiérrez[1], Luz Helena Patiño[1], Luis David Sáenz Pérez[2], Karen Julieth Moreno Medina[2], Juan Carlos Villar Centeno[2], Juan David Ramírez[1,3*]

**Affiliations:**

1- Centro de Investigaciones en Microbiología y Biotecnología-UR (CIMBIUR), Facultad de Ciencias Naturales, Universidad del Rosario, Bogotá, Colombia
2- Fundación Cardio infantil- Instituto de Cardiología, Bogotá, Colombia.
3- Molecular Microbiology Laboratorio, Department of Pathology, Molecular and Cell-based Medicine, Icahn School of Medicine at Mount Sinai, New York, NY, USA

*Corresponding author: juand.ramirez@urosario.edu.co, juan.ramirezgonzalez@mssm.edu

**ABSTRACT**

Chagas disease (CD), caused by the protozoan *Trypanosoma cruzi*, remains a major public health challenge due to limited treatment options, Benznidazole and Nifurtimox; which are associated with adverse effects and variable efficacy. The emergence of drug-resistant in *T. cruzi* strains, along with limited knowledge of the molecular mechanisms underlying resistance, hampers the development of more effective therapies. To explore these mechanisms, we performed a comparative transcriptomic analysis of two *T. cruzi* TcI strains: MG (naturally susceptible) and DA (naturally resistant) to Benznidazole. Parasites were cultured in LIT medium, and EC50 values were determined using the MTT assay. RNA was extracted and sequenced (RNA-seq), with reads aligned to a reference genome. Differential gene expressions were analyzed with DESeq2, functional enrichment through Gene Ontology (GO), and metabolic pathways were mapped via KAAS. The EC50 for Benznidazole in DA (28.92 µg/mL) was substantially higher than in MG (0.8827 µg/mL), confirming differential susceptibility. DA showed 408 upregulated and 1,515 downregulated genes, while MG had 153 upregulated and 866 downregulated (Log2FoldChange ≥ 2 or ≤ -2). GO analysis indicated divergent biological processes between strains: DA exhibited enrichment in electron transport and detoxification, while MG was enriched in DNA repair and energy metabolism. Metabolic mapping revealed significant differences in the pentose phosphate pathway, glycolysis/gluconeogenesis, and the tricarboxylic acid (TCA) cycle. Key genes potentially involved in resistance like prostaglandin F2α synthase, trypanothione synthase, thioredoxin, and prostaglandin F synthase were identified as candidate therapeutic targets. These findings suggest that Benznidazole resistance in *T. cruzi* involves multifactorial, strain-specific responses at the transcriptomic and metabolic levels. By analyzing naturally resistant and susceptible strains, this study provides novel insights into mechanisms of drug resistance and underscores the need for expanded research across genetically diverse *T. cruzi* strains and discrete typing units (DTUs) to inform future therapeutic strategies.

**KEYWORDS:** Chagas disease, Benznidazole, Drug resistance, Transcriptomics, RNA-seq, *Trypanosoma cruzi*, Differential gene expression.

## INTRODUCTION

Chagas disease (CD), caused by *Trypanosoma cruzi*, remains a significant public health concern in the Americas, affecting 7–8 million people and placing an additional 25 million at risk, primarily in Latin America (1–4). Although once geographically restricted, migration has expanded its reach globally (5). The primary mode of transmission is via Triatominae insects, which spread the parasite through their feces. However, *T. cruzi* can also be transmitted through blood transfusion, congenital transmission, organ transplantation, laboratory accidents, and ingestion of contaminated food (3,6–9).

The disease progresses through acute and chronic phases. Although the acute phase is often asymptomatic, it may present with nonspecific symptoms, while the chronic phase can lead to severe cardiac or digestive complications in 30–40% of patients (8). Diagnosis and treatment remain challenging, particularly because chronic manifestations are often detected too late, requiring advanced and costly interventions (4,10,11).

Trypanocidal treatment relies primarily on Benznidazole and Nifurtimox, which are most effective in the acute phase and younger patients (4,12,13). Benznidazole, the more commonly used drug, acts through nitroreduction, binding to parasite DNA and interacting with proteins and lipids (14). However, Benznidazole's effectiveness decreases in chronic cases and is significantly influenced by host-specific factors and parasite strain diversity, which together contribute to variable therapeutic outcomes (15–18). In pediatric populations from Bolivia, Argentina, and Brazil, the drug has been shown to induce serological clearance in 83–97% of patients, providing a strong marker of therapeutic success (16,19). In contrast, observational studies conducted primarily in countries of the Southern Cone, including Argentina and Brazil, have suggested that benznidazole may slow disease progression and reduce the risk of cardiomyopathy by approximately 50% in adults with the indeterminate form of CD, though these findings have not been entirely consistent; however, despite these potential benefits, sustained parasitological cure rates remain low, highlighting the ongoing challenges in achieving lasting remission (20,21).

WHO guidelines recommend treatment for children under 14 and adults under 50 with indeterminate CD, but whether to expand treatment to those with cardiomyopathy remains debated due to limited evidence from clinical trial data (16,21–23). A key limitation in current research is that most adult treatment data come from observational studies rather than clinical trials with clearly defined endpoints. To address this gap, a Phase III clinical trial was launched by DNDi in 2023 in Argentina to evaluate the efficacy of two-week and four-week benznidazole regimens for adults in the chronic phase of the disease. This study aims to validate shorter treatment regimens and provide more robust evidence on therapeutic outcomes in patients without advanced disease. (19). Despite Benznidazole's long-standing use and safety profile, its tolerability is limited by a high incidence of adverse effects, including dermatological (29–50%), gastrointestinal (5–15%), and neurological symptoms (up to 33%), sometimes necessitating treatment discontinuation (4,24–29). The demanding 60-day regimen and frequent monitoring further reduce adherence, particularly in resource-limited settings, where discontinuation rates reach up to 20%. Shorter treatment regimens

may offer the potential for improved tolerability while maintaining comparable efficacy, potentially enhancing patient adherence and overall treatment success. (19,30,31).

Treatment efficacy is also undermined by growing pharmacological resistance in *T. cruzi*, particularly in strains exposed to long-term drug pressure (32,33). Unlike therapeutic failure caused by factors like poor adherence or host variability, resistance is associated with parasite genetics, including DTU classification. Strains from DTU TcI are generally more susceptible, while those from TcII and others DTUs exhibit greater resistance (34–36).

Multiple mechanisms contribute to this resistance, such as enhanced antioxidant defenses (e.g., superoxide dismutase), DNA repair pathways, and mutations in the TcNTR gene, which impairs Benznidazole activation (37,38). Furthermore, resistant strains frequently overexpress genes involved in oxidative stress management, including glutathione transferases and superoxide dismutase (39–41), and show metabolic adaptations in detoxification and energy pathways (42).

Additionally, some *T. cruzi* strains display intrinsic resistance independent of prior drug exposure suggesting the involvement of stable genetic or environmental factors (33,43). While this phenomenon is increasingly recognized, the molecular basis of intrinsic resistance remains poorly understood, emphasizing its importance as a research priority (40,42,44,45).

Transcriptomic approaches have proven value in exploring resistance mechanisms by revealing differential gene expression patterns in resistant strains (44,45). However, most studies have focused on acquired resistance, with limited insight into intrinsic mechanisms (41,42). Although candidate resistance biomarkers have been proposed, a validated method for detecting naturally resistant strains is still lacking, limiting clinical application (42,46–48).

Given the growing concern over resistance in *T. cruzi*, it is critical to understand its strategies *T. cruzi* to evade drug action. In this study, we performed a comparative transcriptomic analysis of a naturally susceptible strain (MG) and a resistant strain (DA) of *T. cruzi* exposed to Benznidazole. Our goal was to identify gene expression patterns associated with resistance to gain a deeper understanding of the molecular adaptations that enable *T. cruzi* to withstand treatment. The findings of this study may contribute to the development of more effective therapeutic strategies for CD.

## MATERIALS AND METHODS

### Biological Material

The strains DA (MHOM/CO/01/DA) and MG (MHOM/CO/04/MG), belonging to the *T. cruzi* DTU TcI, were used, characterized by their resistance and sensitivity to Benznidazole, respectively (49). These strains were thawed from the cryobank of the Microbial Research Group of Universidad del Rosario (GIMUR). After thawing, they were maintained in culture in LIT medium, supplemented with 10% fetal bovine serum (FBS), and incubated at 26 °C, with subcultures every 5 days.

### Calculation of Benznidazole EC50

To determine the EC50 value of Benznidazole in the DA and MG strains, the parasites were cultured in LIT medium for 5 days, and a count was performed using a Neubauer chamber. Subsequently, 1 x $10^6$ parasites/mL were seeded in a 24-well culture plate with serial dilutions of Benznidazole (from 50 µg/mL to 0.19 µg/mL). As a positive control, two wells with 1 x $10^6$ parasites/mL in LIT medium were included, and as a negative control, another two wells with 1 x $10^6$ parasites/mL in LIT medium and hydrogen peroxide to induce cell death. The plate was incubated at 37 °C for 72 hours.

Following incubation, the MTT colorimetric assay from Abcam (https://www.abcam.com/en-us/technical-resources/protocols/mtt-assay) was performed to measure cell viability, and the absorbance results were analyzed using GraphPad Prism 9 software. EC50 value was calculated with these data.

**RNA Sequencing**

After calculating the EC50 concentration, triplicate cultures of the DA and MG strains were performed in LIT medium for 72 hours at 26 °C. To each culture, the corresponding EC50 concentration of Benznidazole for each strain was added, and untreated controls were included for comparison. After incubation, total RNA was extracted from each of the cultures, including the controls, using the Qiagen RNeasy Plus Mini Kit. The extracted RNA was sequenced on the Illumina NovaSeq 6000 platform using Pair-end 150 bp RNA-Seq technology, generating a total of 21.63 GB of data, with a minimum of 20 million reads per sample. The data obtained was stored on the institutional server of Universidad del Rosario for detailed bioinformatic analysis.

**Bioinformatic Pre-processing**

Using the data stored, a transcriptomic analysis that included several key steps was carried out. First, quality control and adapter trimming were performed using the Trimmomatic program (http://www.usadellab.org/cms/?page=trimmomatic), to remove adapters and low-quality bases. For this, the parameters SLIDINGWINDOW:4:20, MINLEN:100, and AVGQUAL:20 were used, ensuring the high quality of the reads for subsequent analysis. Subsequently, the processed reads were aligned to the "*Trypanosoma cruzi* BrazilA4" reference genome (https://tritrypdb.org/tritrypdb/app/search?q=Trypanosoma+cruzi+Brazil+A4), using the STAR software (https://github.com/alexdobin/STAR), configured with specific parameters to maximize alignment accuracy and reduce multiple mapping. In particular, the two-pass Mode Basic alignment mode was activated, which improves accuracy by detecting new junctions in the first pass and applying that information in the second. Additionally, the outFilterMultimapNmax 1 parameter was set to limit the maximum number of loci where a read can be mapped, thus minimizing multiple mapping. Finally, gene expression quantification was performed using the BAM files generated during alignment, with HTSeq (https://github.com/htseq/htseq) in "intersection-nonempty" mode, which counts only the reads that overlap with the genomic annotations.

**Differential Gene Expression Analysis**

A differential gene expression analysis of the DA and MG strains was performed using the DESeq2 package (https://github.com/thelovelab/DESeq2) in the R statistical software (Version 4.4.1). To achieve this, we loaded the gene count data obtained from the previous HTSeq analysis and created a DESeqDataSet object. Subsequently, we filtered this data to remove genes exhibiting low counts in at least one sample group. The differential analysis was carried out between the C1 (Control) and C2 (Strain exposed to Benznidazole) conditions for both strains, using a negative binomial generalized linear model implemented in DESeq2, with a design that included the condition as an explanatory variable. The results were filtered to include only differentially expressed genes with an adjusted p-value (padj) less than 0.05 and a Log2FoldChange ≥ 2 or ≤ -2. For the visualization and validation of the results, various graphs were generated as follows: principal component analyses (PCAs) using ggplot2 (https://ggplot2.tidyverse.org/), volcano plots using the EnhancedVolcano package (https://github.com/kevinblighe/EnhancedVolcano), Venn diagrams using the InteractiVenn online tool (https://www.interactivenn.net/), and heatmaps using the pheatmap package (https://github.com/raivokolde/pheatmap).

**Functional Enrichment Analysis (GO) and Metabolic Pathways**

A functional enrichment analysis was performed using the Gene Ontology (GO) database hosted on TriTrypDB (https://tritrypdb.org/tritrypdb/app), to identify biological processes (BP), cellular components (CC), and molecular functions (MF) enriched in the differentially expressed genes. The results were visually represented using enrichment bubble plots. Additionally, the KAAS (KEGG Automatic Annotation Server) online tool (https://www.genome.jp/kaas-bin/kaas_main) was used to assign the sequences of the upregulated and downregulated genes of the DA and MG strains in the context of specific *T. cruzi* metabolic pathways.

**RESULTS**

**EC50 Calculation and RNA Sequencing**

The EC50 calculation, defined as the Benznidazole concentration required to inhibit 50% of parasite growth, revealed that the DA strain had an EC50 of approximately 28.92 µg/mL, while the MG strain showed an EC50 of 0.8827 µg/mL (**Supplementary Figure 1**). This indicates that the MG strain is susceptible to Benznidazole compared to the DA strain.

After calculating the EC50 concentration for each strain, they were exposed *in vitro* to these drug concentrations, and total RNA was extracted and subsequently sequenced. The quality and quantity of the extracted RNA were satisfactory in all samples, with yields exceeding 200 ng/µL and an A260/A280 ratio close to 2.0, confirming RNA purity. Sequencing was performed using the Illumina paired end 150 bp platform, yielding a minimum of 20 million reads per sample. The data exhibited high accuracy, with an average Phred quality score exceeding 30, reflecting the overall reliability and fidelity of the sequencing output.

**Differential Gene Expression Analysis**

To assess the global variation in gene expression, a principal component analysis (PCA) was first conducted for each strain, comparing control and Benznidazole-treated samples. The PCA plots capture most of the variation in the dataset: 84.1% for the DA strain (**Figure 1A**) and 82% for the MG strain (**Figure 1B**), based on the first two principal components. Specifically, the DA strain shows 72.3% and 11.8% variance along PC1 (X-axis) and PC2 (Y-axis), respectively, while the MG strain shows 69.4% and 12.6%. In both strains, the PCA revealed a clear separation between control (burgundy) and treated (olive green) samples, indicating substantial transcriptional reprogramming in response to Benznidazole. The spread of samples along PC1 suggests this component is sufficient to distinguish treated from untreated conditions, regardless of the strain's susceptibility.

Subsequently, using the DESeq2 package in R, 13,725 differentially expressed genes were identified in the DA strain and 13,701 in the MG strain, both with an adjusted P-value ≤ 0.05. Among these genes, 6,940 upregulated and 6,785 downregulated genes were identified in the DA strain, while 6,892 upregulated and 6,809 downregulated genes were found in the MG strain.

After performing PCA and differential gene expression analyses, a Venn diagram and various Volcano plots were generated, representing differentially expressed genes, filtering for genes with a Log2foldchange ≥ 2 and ≤ -2. The DA strain showed 408 upregulated and 1,515 downregulated genes (**Figure 1C and 1E**), while the MG strain showed 153 upregulated and 866 downregulated genes (**Figure 1D and 1E**). These results suggest a strain-specific transcriptomic response upon Benznidazole exposure. However, shared genes between both strains were also identified (**Figure 1E**), indicating that certain cellular processes respond to the drug in a conserved manner. Precisely, it was observed that 99 genes exhibited upregulation and 718 genes showed downregulation in both strains.

**Functional Annotation of Genes**

Successively, functional annotation of up and downregulated genes (with Log2FoldChange ≤ 2 and ≥ 2, respectively) for the DA and MG strains (**Figure 1**) was performed using the TriTrypDB database. A total of 1,314 genes for the DA strain and 723 genes for the MG strain were identified. Additionally, 609 genes and 296 genes were assigned as hypothetical proteins without predicted function for the DA and MG strains, respectively. Finally, to provide a more focused perspective on differential gene expressions in the DA and MG strains, a heatmap was constructed with the 20 genes with the highest and 20 with the lowest Log2foldchange (**Figure 2**).

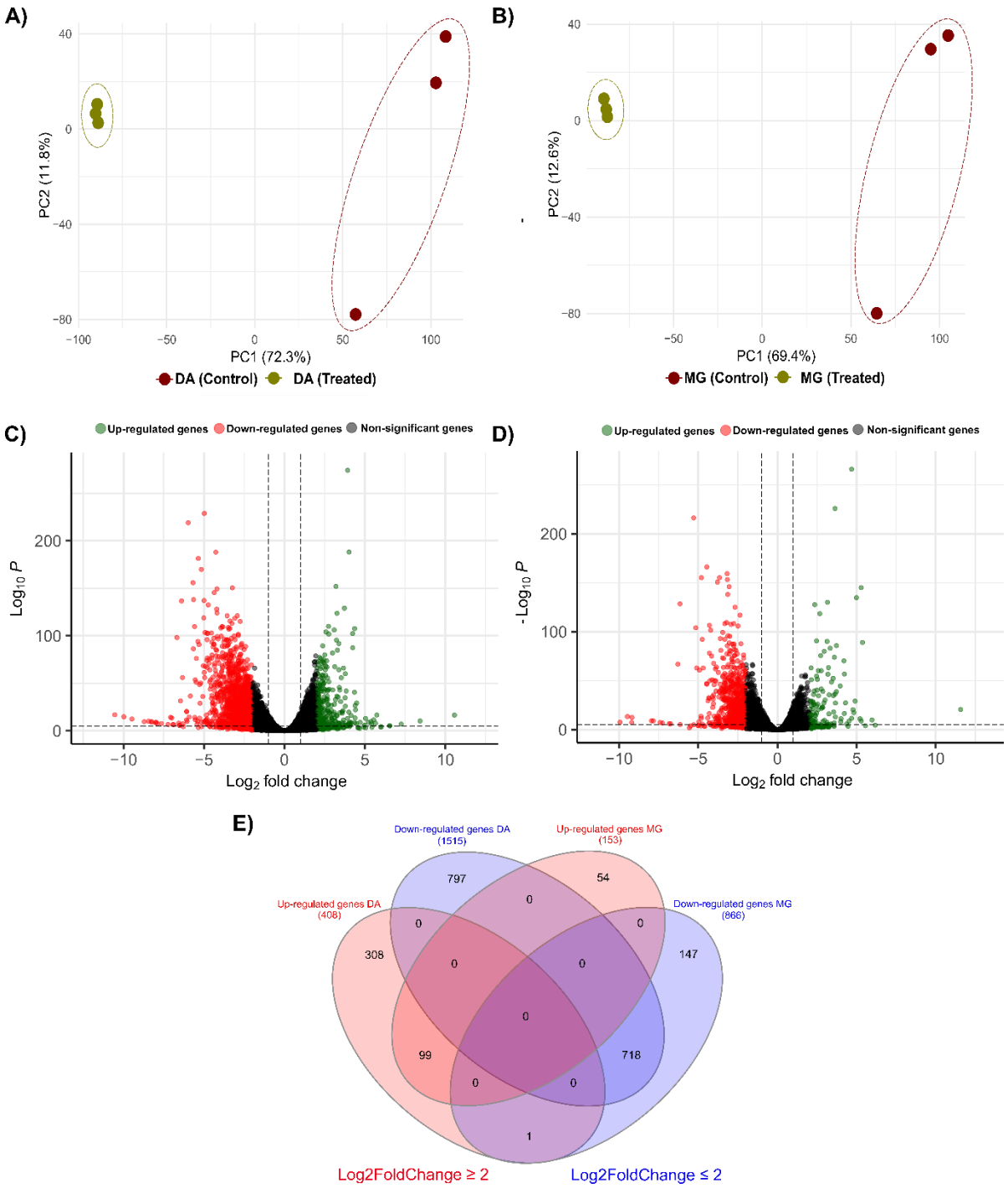


**Figure 1.** Gene expression analysis in DA and MG strains after Benznidazole treatment. (**A**) Principal Component Analysis (PCA) of the DA strain under control and post-treatment conditions. The spatial distribution of points in the principal component space reveals a clear separation between treated and untreated samples, indicating significant alterations in gene expression following Benznidazole exposure. (**B**) Principal Component Analysis (PCA) of the MG strain, comparing control and post-treatment conditions. Like the DA strain, a well-defined segregation between sample groups is observed, suggesting a distinct

transcriptional response to Benznidazole. (**C**) Volcano plot for the DA strain, representing the distribution of 13,725 differentially expressed genes. Red points indicate significantly downregulated genes ($Log_2$FoldChange ≤ 2), green points correspond to upregulated genes ($Log_2$FoldChange ≥ 2), and black points represent genes with no significant expression changes. (**D**) Volcano plot for the MG strain, displaying 13,701 differentially expressed genes, following the same color representation as in the DA strain. Notable differences in the quantity and magnitude of regulated genes highlight a strain-specific response to Benznidazole, further underscoring the genetic variability in *T. cruzi* and its influence on drug susceptibility. (**E**) Venn diagram displaying the total number of differentially expressed genes in both strains, distinguishing between upregulated ($Log_2$FoldChange ≥ 2) and downregulated ($Log_2$FoldChange ≤ 2) genes.

Among the most prominent upregulated genes were those encoding putative proteins like kinesins, retrotransposon hot spot (RHS) proteins, transialidases, and small GTP-binding proteins RAB6 in the DA strain (**Figure 2A**). For the MG strain, genes encoding proteins like kinesins, retrotransposon hot spot (RHS) proteins, zinc finger proteins, and phosphatase 2C-like proteins were also identified (**Figure 2B**) (**Supplementary Table 1 & 2)**.

Furthermore, among the most relevant downregulated genes were those encoding pteridine reductase 2 (ptr2), elongation factor 1-alpha (EF-1α), surface proteases GP63, and CMGC/DYRK protein kinases in the DA strain (**Figure 2A**); while in the MG strain, genes encoding surface proteases GP63, CMGC/DYRK protein kinases, aspartyl-tRNA synthetase, and D-isomer-specific 2-hydroxyacid dehydrogenase were prominent (**Figure 2B**). Differences in expression patterns between both strains suggest that the Benznidazole response involves modulating specific metabolic pathways, and genes responsible for these differences may be directly associated with drug resistance mechanisms in these strains.

**Functional Enrichment (GO) of Genes**

The GO analysis identified 126 upregulated and 53 downregulated terms in the DA strain, and 40 upregulated and 91 downregulated terms in the MG strain. Notably, for the MG strain, no GO terms were retrieved in the cellular component category due to the limited number of upregulated genes ($Log_2$FoldChange ≥ 2) falling below the statistical significance threshold for enrichment analysis (P-value cutoff = 0,05). An enrichment graph (**Figure 3**) was generated to display the top 30 GO terms with the highest number of associated genes in both strains, along with the percentage of differentially expressed genes within each category. Figures **3A** and **3B** display the upregulated and downregulated GO terms for the DA strain, respectively, while Figures **3C** and **3D** present the corresponding GO terms for the MG strain, covering all three GO domains: biological process, molecular function, and cellular component. Overall, GO analysis revealed that the differentially expressed genes in both strains are involved in a wide range of essential biological functions. Upregulated genes were predominantly associated with pathogenesis, catalytic activity, and cellular organization, while downregulated genes were mainly linked to metabolic processes, cell adhesion, and ribosomal functions.

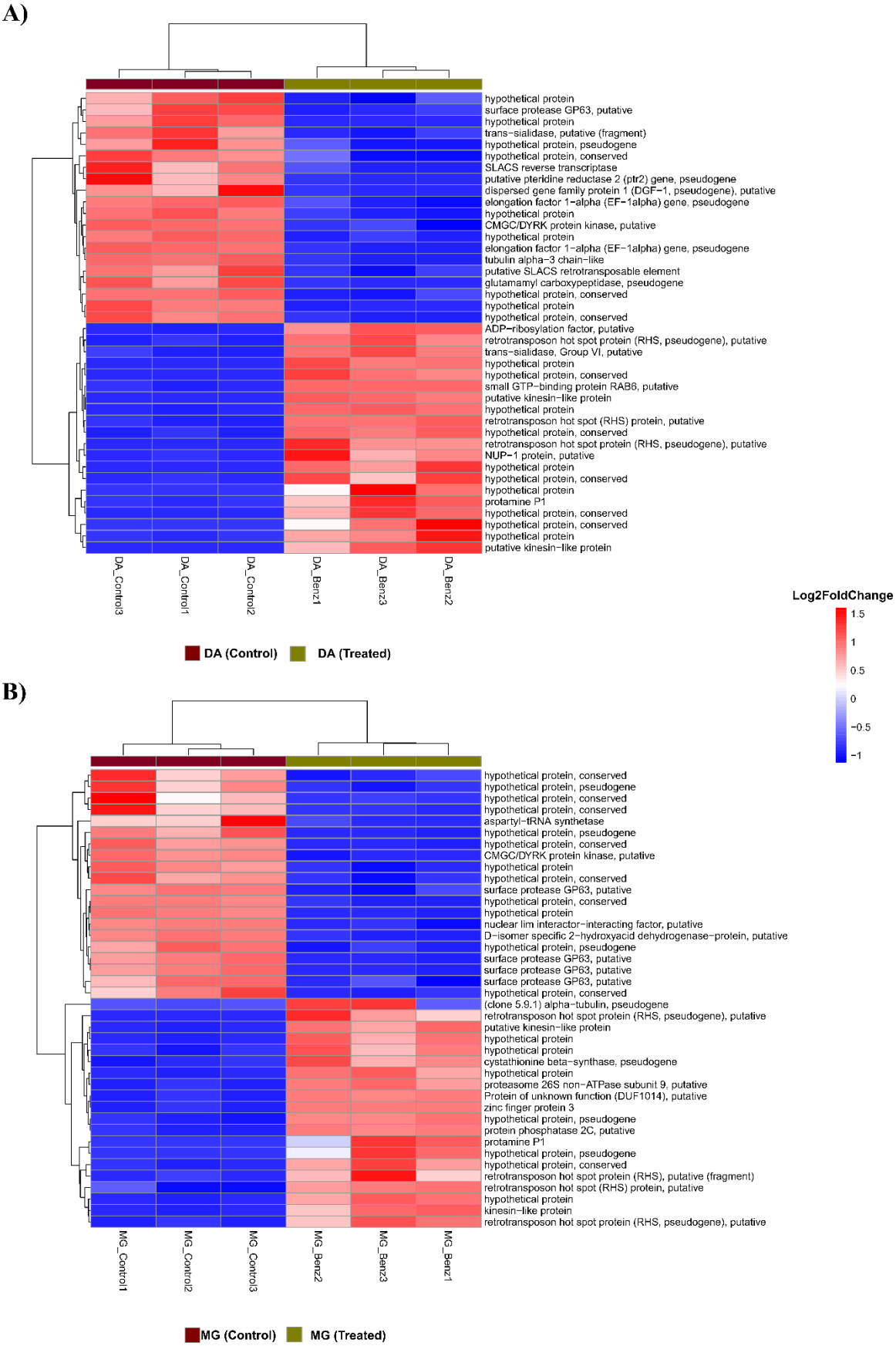
A)
hypothetical protein
surface protease GP63, putative
hypothetical protein
trans−sialidase, putative (fragment)
hypothetical protein, pseudogene
hypothetical protein, conserved
SLACS reverse transcriptase
putative pteridine reductase 2 (ptr2) gene, pseudogene
dispersed gene family protein 1 (DGF−1, pseudogene), putative
elongation factor 1−alpha (EF−1alpha) gene, pseudogene
hypothetical protein
CMGC/DYRK protein kinase, putative
hypothetical protein
elongation factor 1−alpha (EF−1alpha) gene, pseudogene
tubulin alpha−3 chain−like
putative SLACS retrotransposable element
glutamamyl carboxypeptidase, pseudogene
hypothetical protein, conserved
hypothetical protein
hypothetical protein, conserved
ADP−ribosylation factor, putative
retrotransposon hot spot protein (RHS, pseudogene), putative
trans−sialidase, Group VI, putative
hypothetical protein
hypothetical protein, conserved
small GTP−binding protein RAB6, putative
putative kinesin−like protein
hypothetical protein
retrotransposon hot spot (RHS) protein, putative
hypothetical protein, conserved
retrotransposon hot spot protein (RHS, pseudogene), putative
NUP−1 protein, putative
hypothetical protein
hypothetical protein, conserved
hypothetical protein
protamine P1
hypothetical protein, conserved
hypothetical protein, conserved
hypothetical protein
putative kinesin−like protein
DA_Control3
DA_Control1
DA_Control2
DA_Benz1
DA_Benz3
DA_Benz2
DA (Control)
DA (Treated)
Log2FoldChange
1.5
1
0.5
0
−0.5
−1
B)
hypothetical protein, conserved
hypothetical protein, pseudogene
hypothetical protein, conserved
hypothetical protein, conserved
aspartyl−tRNA synthetase
hypothetical protein, pseudogene
hypothetical protein, conserved
CMGC/DYRK protein kinase, putative
hypothetical protein
hypothetical protein, conserved
surface protease GP63, putative
hypothetical protein, conserved
hypothetical protein
nuclear lim interactor−interacting factor, putative
D−isomer specific 2−hydroxyacid dehydrogenase−protein, putative
hypothetical protein, pseudogene
surface protease GP63, putative
surface protease GP63, putative
surface protease GP63, putative
hypothetical protein, conserved
(clone 5.9.1) alpha−tubulin, pseudogene
retrotransposon hot spot protein (RHS, pseudogene), putative
putative kinesin−like protein
hypothetical protein
hypothetical protein
cystathionine beta−synthase, pseudogene
hypothetical protein
proteasome 26S non−ATPase subunit 9, putative
Protein of unknown function (DUF1014), putative
zinc finger protein 3
hypothetical protein, pseudogene
protein phosphatase 2C, putative
protamine P1
hypothetical protein, pseudogene
hypothetical protein, conserved
retrotransposon hot spot protein (RHS), putative (fragment)
retrotransposon hot spot (RHS) protein, putative
hypothetical protein
kinesin−like protein
retrotransposon hot spot protein (RHS, pseudogene), putative
MG_Control1
MG_Control2
MG_Control3
MG_Benz2
MG_Benz3
MG_Benz1
MG (Control)
MG (Treated)

**Figure 2.** Heatmap of the 20 genes with the highest differential expression (Log2FoldChange) in DA and MG TCI strains treated with Benznidazole. The heatmap visualizes expression levels of the 20 genes showing the greatest differences in expression between DA (**A**) and MG (**B**) TCI strains. Colors represent the change in gene expression (Log2FoldChange), where red indicates increased expression and blue indicates decreased expression. Rows correspond to different genes, and columns to different replicates for both DA and MG strains.

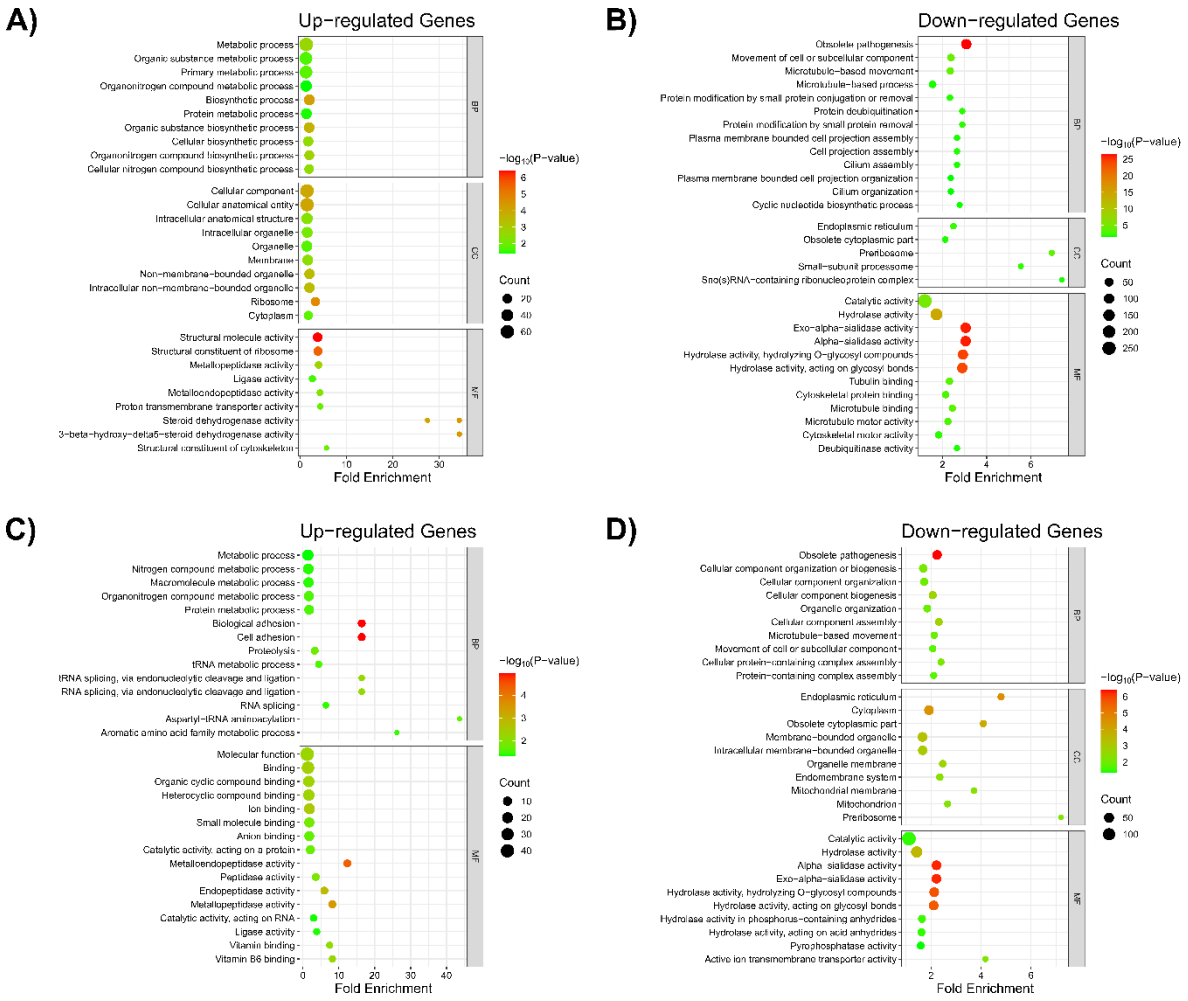


**Figure 3.** Gene ontology enrichment analysis in DA and MG strains. Gene ontology (GO) enrichment analysis was performed to identify over-represented biological processes (BP), cellular components (CC), and molecular functions (MF) in differentially expressed genes of DA and MG strains. Graphs show the most significant GO terms, with point size corresponding to the number of annotated genes and color intensity reflecting the adjusted P-value, indicating statistical significance. The x-axis represents the frequency of annotated genes for each GO term, while the y-axis classifies GO terms by significance. Panels are organized as follows: **A** and **B**, positively and negatively regulated genes in the DA strain, respectively; **C** and **D**, positively and negatively regulated genes in the MG strain, respectively.

## Metabolic Pathway Analysis

We identified three metabolic pathways with the highest number of involved genes in both strains (**Figure 4**): the pentose phosphate pathway (PPP), glycolysis/gluconeogenesis, and the citrate cycle (TCA). In the pentose phosphate pathway (**Figure 4A**), 6-phosphogluconolactonase, deoxyribose-phosphate aldolase, and a phosphomannomutase-like protein genes were detected in the DA strain, while only the latter two were found in the MG strain. In glycolysis/gluconeogenesis (**Figure 4B**), the DA strain showed phosphomannomutase-like protein and phosphoglycerate kinase genes, while the MG strain also identified pyruvate phosphate dikinase and dihydrolipoyl dehydrogenase. Finally, in the citrate cycle (**Figure 4C**), both strains have two genes, albeit with differences: DA expresses isocitrate dehydrogenase [NADP] and cytosolic malate dehydrogenase, while MG has cytosolic malate dehydrogenase and dihydrolipoyl dehydrogenase. These results reveal variations in gene expression between the DA and MG strains, potentially influencing their metabolism and response to treatment.

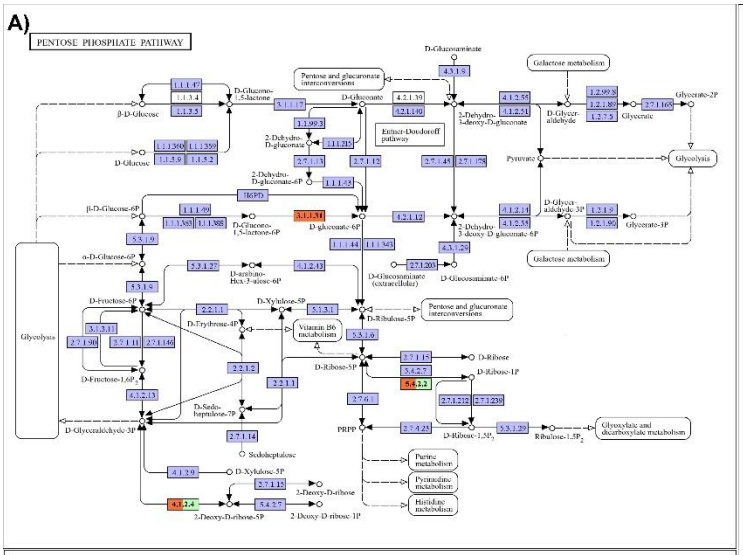


| Gene code | Description |
|---|---|
| 1.1.1.37 | Cytosolic malate dehydrogenase, putative |
| 1.1.1.42 | Isocitrate dehydrogenase [NADP], mitochondrial precursor, putative |
| 1.8.1.4 | Dihydrolipoyl dehydrogenase, putative |
| 2.7.2.3 | Phosphoglycerate kinase, putative |
| 2.7.9.1 | Pyruvate phosphate dikinase, pseudogene |
| 3.1.1.31 | 6-phosphogluconolactonase, putative |
| 4.1.2.4 | Deoxyribose-phosphate aldolase, putative |
| 5.4.2.2 | Phosphomannomutase-like protein, putative |

**Figure 4.** DA and MG strain genes involved in metabolic pathways (glycolysis/gluconeogenesis, pentose phosphate, and citrate cycle). Figures show graphical representations of three key metabolic pathways in *T. cruzi*: pentose phosphate (**A**), glycolysis/gluconeogenesis (**B**), and citrate cycle (TCA) (**C**). The Pentose phosphate pathway involves 3 genes in the DA strain and 2 in the MG strain. For glycolysis/gluconeogenesis, 2 genes were identified in the DA strain, while 4 genes were found in the MG strain. In the citrate cycle, both strains have 2 genes involved. Orange codes represent genes from the DA strain, and green codes correspond to genes from the MG strain. The table shows the code and description of DA and MG strain genes involved in different metabolic pathways.

## DISCUSSION

Despite being discovered over a century ago, CD continues to be neglected, primarily due to limitations in early diagnosis and a lack of effective, well-tolerated therapeutic options (1,42). Currently, Benznidazole and Nifurtimox are the only drugs available for clinical treatment. However, their therapeutic utility is significantly compromised by frequent and severe side effects, along with limited efficacy especially during the chronic phase of the disease (50,51). The complexity is further compounded by the emergence of drug-resistant strains of *T. cruzi*, which utilize diverse molecular mechanisms to evade the effects of these nitroheterocyclic compounds, thereby complicating eradication efforts and exacerbating disease burden (50,51).

One of the proposed mechanisms for Benznidazole resistance in *T. cruzi* involves a reduction in the generation of toxic free radicals, typically produced through nitroreduction of the drug within the parasite (27). Alterations in drug transporter activity and the upregulation of DNA repair pathways are also thought to contribute to this resistance phenotype (40,42). Although advances have been made in identifying genes and pathways potentially involved in these responses, the precise molecular basis remains poorly understood. Most previous studies have relied on resistance models developed through in vitro selection, which may not accurately reflect the complexity and diversity of naturally occurring strains.

In contrast to artificially selected models, our study adopts a novel strategy by investigating the natural variability of *T. cruzi*. We directly compare strains with inherent resistance or susceptibility to Benznidazole, providing a more physiologically relevant context for elucidating the mechanisms underpinning resistance. By focusing on transcriptomic differences between naturally resistant and susceptible strains, we aim to uncover core regulatory networks and metabolic pathways that define the differential response to drug exposure. This approach allows for a more holistic understanding of resistance mechanisms and reveals adaptive strategies that may remain hidden in laboratory-induced models. Ultimately, our findings have the potential to inform the development of more effective treatment regimens and contribute to the identification of novel therapeutic targets for CD (42,52).

Our comparative transcriptomic analysis of *T. cruzi* DA and MG strains following Benznidazole treatment reveals extensive gene expression divergences, suggesting the presence of pre-existing, strain-specific mechanisms of drug response (**Figure 1**). Rather

than being a consequence of general drug-induced alterations, these transcriptional differences appear to reflect deep-rooted genetic and regulatory adaptations. This finding is consistent with broader observations in parasitology, where complex gene regulatory shifts often underpin resistance to chemotherapeutic agents (53–55). Notably, our analysis highlights the enrichment of genes involved in amino acid metabolism, translation, DNA repair, and redox homeostasis functions that are likely to represent active survival strategies rather than passive stress responses (42,56). These enriched categories not only corroborate previous research but also extend current understanding by linking them to natural resistance phenotypes.

Interestingly, genes related to energy metabolism were found to be upregulated in the resistant DA strain, paralleling findings from Cunha-Neto et al. (2005) in chronic chagasic cardiomyopathy patients, where metabolic rewiring was associated with disease progression and parasite persistence (57). This convergence suggests that metabolic flexibility may be a hallmark of *T. cruzi* strains capable of enduring drug-induced oxidative stress. These inherent differences in metabolic regulation and stress response capacity point to sophisticated parasite adaptations and emphasize the need to investigate these processes further as potential drug targets. Together, these findings reveal a complex and multifaceted network of resistance mechanisms in Benznidazole-resistant *T. cruzi* strains, emphasizing that resistance is not monogenic but rather the result of coordinated alterations across multiple cellular pathways. Importantly, these resistance strategies are closely linked to the specific mechanisms of action of Benznidazole, highlighting the challenge of overcoming drug resistance in this pathogen.

The transcriptomic profiles of the DA and MG strains underscore the distinct molecular strategies deployed by each strain in response to Benznidazole. In the DA strain, upregulation of DNA repair genes and those involved in reactive oxygen species (ROS) detoxification highlights an enhanced capacity to manage drug-induced genotoxicity. These findings support the growing consensus that Benznidazole resistance involves not only altered drug activation but also improved cellular mechanisms for damage mitigation (42,58,59). Crucially, these gene expression differences are not ephemeral consequences of drug stress but likely represent intrinsic adaptations embedded within the MG strain's regulatory architecture.

To substantiate this hypothesis, future studies must include functional validation of differentially expressed genes. Gene silencing and overexpression studies especially using advanced CRISPR/Cas9 gene editing systems could definitively establish causal links between gene function and drug susceptibility. CRISPR-based techniques have already been successfully employed in other trypanosomatids and represent a powerful avenue for dissecting resistance pathways in *T. cruzi* (60). For instance, targeting DNA repair enzymes or antioxidant genes in resistant strains could reveal how their modulation impacts Benznidazole sensitivity. Recent work by Mejía-Jaramillo et al. (2025) has already demonstrated that alterations in nitroreductase I (NTRI), a key enzyme in drug activation, can confer resistance, further reinforcing the value of such functional approaches (61).

Our gene expression data align with earlier observations from García-Huertas et al. (2017a), who identified over 130 differentially expressed genes in a naturally resistant strain, many of which were involved in metabolic functions, catalysis, transport, and redox balance (42,43,54,62,63). In our study, the DA strain exhibits high expression of prostaglandin F2α synthase, a gene previously linked to increased Benznidazole sensitivity and oxidative stress management (62,64). Similarly, upregulation of trypanothione synthetase, a key enzyme in thiol-based detoxification, aligns with findings from Mejía et al. (2025), suggesting a prominent role in neutralizing ROS and promoting parasite survival (61,65).

Beyond these, thioredoxin was also significantly upregulated in the DA strain, supporting its role in redox regulation. As part of the thioredoxin system, this protein contributes to selenium metabolism and maintains glutathione peroxidase activity, which collectively form a robust antioxidant defense. The ability to mitigate host and drug induced oxidative damage may be decisive for parasite survival under chemotherapeutic pressure (42,66). The DA strain also showed higher expression of prostaglandin F synthase, whose role in modulating oxidative stress responses and infectivity has been highlighted by Santi et al. (2022). Despite contrasting findings by Lima et al. (2023), the current results point to a nuanced, context-dependent role for this enzyme in resistance (42,66,67).

Paradoxically, several stress related genes were downregulated in the DA strain. For instance, Aldo-keto reductase, which has been previously associated with resistance to Benznidazole and glyoxal, was significantly suppressed, diverging from findings by González et al. (2017b) (68). Similarly, heat shock proteins crucial in protein folding and cellular stress responses—were predominantly downregulated, suggesting a departure from canonical stress adaptation pathways (61,69). Downregulation of nitroreductase, a well-established determinant of Benznidazole activation, further complicates the resistance profile of this strain. Reduced expression of this enzyme has been associated with diminished drug activation and increased resistance, highlighting the strain-specific nature of these adaptations (42,70).

In contrast, in the MG strain, notable downregulation of genes encoding kinesins and motor proteins suggests impaired intracellular transport and cell division, which may affect replication under stress conditions and contribute to differential drug sensitivity (71). This observation echoes findings from Zingales and Macedo (2023), who documented considerable genetic variability among *T. cruzi* strains and their divergent drug responses (43). Further supporting the MG strain's altered redox strategy is the downregulation of glutaredoxin and thioredoxin, both integral to antioxidant defense. These changes reflect a different resistance blueprint that is less reliant on redox buffering and more dependent on DNA repair pathways or metabolic shifts (42,66).

The complexity of Benznidazole resistance in *T. cruzi* is evident in our findings. Rather than being orchestrated by a single master regulator, resistance appears to emerge from polygenic interactions and multilayered physiological adaptations (61,62). This concept is reinforced by GO enrichment analysis, which revealed that the DA strain showed significant upregulation of genes involved in oxidative phosphorylation, the electron transport chain, and nitrogen compound metabolism. These functional enrichments suggest a profound

metabolic reconfiguration that likely facilitates parasite survival during drug exposure (**Figure 3A**) (72,73).

Conversely, the MG strain displayed enrichment of DNA repair processes and cellular mechanisms associated with genome stability, offering an alternative mode of adaptation to drug-induced genotoxic stress (**Figure 3C**) (4). These differences mirror observations by Lima et al. (2023), who reported that resistant strains exhibit wide-ranging alterations in processes such as amino acid metabolism, RNA modification, lipid biosynthesis, and protein folding (42). To further unravel the contribution of these processes, future studies should include functional assessments of genes involved in oxidative metabolism, DNA repair, and redox homeostasis using CRISPR/Cas9 and induced resistance models. Comparative transcriptomics across multiple strains and DTUs will also help delineate the generalizability of these mechanisms.

Additional insights were obtained through pathway analysis using the KAAS, which highlighted upregulation of the PPP, glycolysis-gluconeogenesis, and the TCA cycle in both DA and MG strains (**Figure 4**). The PPP plays a critical role in generating NADPH, an essential cofactor in redox homeostasis, while glycolysis and the TCA cycle support energy demands under oxidative stress (41,42,50). These metabolic adaptations may provide an evolutionary advantage to naturally resistant strains by enhancing their ability to endure hostile, drug induced environments (74,75). A comprehensive analysis integrating transcriptomic, proteomic, and metabolomic data is essential to fully understand the functional significance of these pathways in drug resistance.

Despite the relevance of our findings, several limitations must be acknowledged. First, the transcriptomic analyses were conducted using only two *T. cruzi* strains, which may constrain the broader applicability of our findings, particularly across the parasite's extensive genetic diversity. Second, both strains analyzed are known to exhibit natural resistance and susceptibility to Benznidazole, which limits the generalization of our findings to this specific drug. Moreover, as the strains were obtained from a biological repository and not directly from patients with confirmed post-treatment parasitemia, the clinical relevance of the observed expression profiles may be attenuated. Third, the study employed a single concentration of Benznidazole, restricting insights into potential dose dependent transcriptomic responses. Fourth, the transcriptomic profiling was limited to a specific life stage of *T. cruzi*, without assessing gene expression changes across its complex developmental cycle, which may also impact drug susceptibility. Finally, the absence of whole genome sequencing precludes discrimination between stable genomic variants and transient transcriptional changes (60). Future studies should seek to overcome these limitations by analyzing multiple strains across different DTUs, using a range of drug concentrations, incorporating clinical isolates, and integrating genomic and transcriptomic data across various developmental stages to obtain a more comprehensive understanding of drug resistance mechanisms.

Our RNA-seq analyses reveal that natural Benznidazole resistance in *T. cruzi* may involve more complex, long-term adaptations compared to laboratory-induced resistance. These adaptations likely include evolutionarily entrenched regulatory networks that differ across

DTUs. Cross-comparisons with other transcriptomic studies support the hypothesis that Benznidazole resistance is a multigenic trait influenced by strain-specific factors and DTU membership (42,61,62,68). Nonetheless, several candidate genes such as prostaglandin F2α synthase, trypanothione synthetase, thioredoxin, and prostaglandin F synthase emerge as promising targets for further study. These genes may serve not only as biomarkers of resistance but also as novel therapeutic targets for combination treatments aimed at overcoming drug resistance.

In Colombia, where TcI is the predominant and highly prevalent DTU (76), understanding the molecular determinants of resistance is particularly urgent. This knowledge could inform region-specific treatment strategies and guide public health interventions. To achieve this, large-scale comparative studies across multiple DTUs are essential. Validating key metabolic and signaling pathways through integrative omics approaches brings us closer to implementing precision medicine strategies tailored to *T. cruzi* infection, enabling more targeted and effective therapeutic interventions based on the molecular characteristics of both the parasite and the host.

This study offers valuable insights into the transcriptomic architecture underlying natural Benznidazole resistance in *T. cruzi*, revealing that drug resistance is a complex, multigenic phenomenon shaped by diverse and strain-specific adaptive responses. By comparing two naturally distinct strains, one resistant (DA) and one susceptible (MG), we were able to characterize differential expression patterns across key metabolic, redox, and DNA repair pathways, many of which appear to be constitutively regulated rather than solely induced by drug exposure (**Supplementary Figure 2**). These findings suggest that resistance in naturally circulating strains may stem from long-term evolutionary pressures rather than short-term selective events, as is often the case in *in vitro* models. This distinction is critical for the identification of clinically relevant resistance mechanisms and may help explain the limited success of current chemotherapies in field settings.

Our results further emphasize the importance of integrating transcriptomic data with functional assays and genome-wide analyses to validate the role of candidate genes such as prostaglandin F2α synthase, thioredoxin, and trypanothione synthetase. These genes not only emerge as potential biomarkers of resistance but also represent promising targets for the development of adjunctive or combination therapies aimed at overcoming current pharmacological limitations. Moreover, understanding the molecular underpinnings of resistance in dominant DTUs such as TcI, prevalent in Colombia and much of Latin America, has direct implications for improving clinical management and shaping public health strategies tailored to regional epidemiological contexts. Ultimately, this study contributes to a growing body of evidence that positions comparative transcriptomics as a powerful tool in the fight against CD, offering a roadmap toward precision medicine and more effective, targeted interventions.

**REFERENCES**


1. Organización Mundial de la salud. La enfermedad de Chagas (tripanosomiasis americana). 2023.

2. Ramírez JC, Cura CI, Da Cruz Moreira O, Lages-Silva E, Juiz N, Velázquez E, et al. Analytical validation of quantitative real-time PCR methods for quantification of trypanosoma cruzi DNA in blood samples from chagas disease patients. Journal of Molecular Diagnostics. 2015;17(5):605–15.

3. Ramírez JD, Guhl F, Rendón LM, Rosas F, Marin-Neto JA, Morillo CA. Chagas cardiomyopathy manifestations and trypanosoma cruzi genotypes circulating in chronic chagasic patients. PLoS Negl Trop Dis. 2010 Nov;4(11).

4. Rassi A, Rassi A, Marin-Neto JA. Chagas disease. Vol. 375, The Lancet. Elsevier B.V.; 2010. p. 1388–402.

5. Olivera MJ, Fory JA, Porras JF, Buitrago G. Prevalence of Chagas disease in Colombia: A systematic review and meta-analysis. Vol. 14, PLoS ONE. Public Library of Science; 2019.

6. Cantillo-Barraza O, Torres J, Hernández C, Romero Y, Zuluaga S, Correa-Cárdenas CA, et al. The potential risk of enzootic Trypanosoma cruzi transmission inside four training and re-training military battalions (BITER) in Colombia. Parasit Vectors. 2021 Dec 1;14(1).

7. Hernández C, Salazar C, Brochero H, Teherán A, Buitrago LS, Vera M, et al. Untangling the transmission dynamics of primary and secondary vectors of Trypanosoma cruzi in Colombia: Parasite infection, feeding sources and discrete typing units. Parasit Vectors. 2016 Jan 12;9(1).

8. Pérez-Molina JA, Molina I. Chagas disease. Vol. 391, The Lancet. Lancet Publishing Group; 2018. p. 82–94.

9. Ramírez JD, Guhl F, Umezawa ES, Morillo CA, Rosas F, Marin-Neto JA, et al. Evaluation of adult chronic Chagas' heart disease diagnosis by molecular and serological methods. J Clin Microbiol. 2009;47(12):3945–51.

10. Bern C, Montgomery SP, Herwaldt BL, Rassi A, Marin-Neto JA, Dantas RO, et al. Evaluation and Treatment of Chagas Disease in the United States A Systematic Review. JAMA [Internet]. 2007;298(18):2171–81. Available from: http://jama.jamanetwork.com/

11. Tarleton RL, Gürtler RE, Urbina JA, Ramsey J, Viotti R. Chagas Disease and the London Declaration on Neglected Tropical Diseases. PLoS Negl Trop Dis. 2014;8(10).

12. Fabbro DL, Streiger ML, Arias ED, Bizai ML, Del Barco M, Amicone NA. Trypanocide treatment among adults with chronic Chagas disease living in Santa Fe city (Argentina), over a mean follow-up of 21 years: parasitological, serological and clinical evolution. Rev Soc Bras Med Trop. 2007;(40):1–10.

13. Viotti R, Vigliano C, Lococo B, Bertocchi G, Petti M, María ;, et al. Long-Term Cardiac Outcomes of Treating Chronic Chagas Disease with Benznidazole versus No Treatment A Nonrandomized Trial [Internet]. 2006. Available from: www.annals.org

14. Coura JR. Present situation and new strategies for Chagas disease chemotherapy-a proposal. 2009;104:549–54.

15. Clayton J. Chagas disease: pushing through the pipeline. Nature. 2010;465(Suppl 7301):S12–5.

16. Crespillo-Andújar C, Comeche B, Hamer DH, Arevalo-Rodriguez I, Alvarez-Díaz N, Zamora J, et al. Use of benznidazole to treat chronic Chagas disease: An updated systematic review with a meta-analysis. PLoS Negl Trop Dis. 2022 May 1;16(5).

17. Lascano F, García Bournissen F, Altcheh J. Review of pharmacological options for the treatment of Chagas disease. Vol. 88, British Journal of Clinical Pharmacology. John Wiley and Sons Inc; 2022. p. 383–402.

18. Martín-Escolano J, Medina-Carmona E, Martín-Escolano R. Chagas Disease: Current View of an Ancient and Global Chemotherapy Challenge. Vol. 6, ACS Infectious Diseases. American Chemical Society; 2020. p. 2830–43.

19. DNDi. New benznidazole regimens [Internet]. 2025 [cited 2025 Apr 1]. Available from: https://dndi.org/research-development/portfolio/new-benz-regimens/

20. Rassi A, Grimshaw A, Sarwal A, Sah R, Shah S, Agudelo Higuita NI, et al. Impact of antiparasitic therapy on cardiovascular outcomes in chronic Chagas disease. A systematic review and meta-analysis. EClinicalMedicine. 2025 Jan 1;79.

21. Hasslocher-Moreno AM, Saraiva RM, Sangenis LHC, Xavier SS, de Sousa AS, Costa AR, et al. Benznidazole decreases the risk of chronic Chagas disease progression and cardiovascular events: A long-term follow up study. EClinicalMedicine. 2021 Jan 1;31.

22. Meymandi S, Hernandez S, Park S, Sanchez DR, Forsyth C. Treatment of Chagas Disease in the United States. Curr Treat Options Infect Dis. 2018 Sep;10(3):373–88.

23. Viotti R, Alarcón De Noya B, Araujo-Jorge T, Grijalva MJ, Guhl F, López MC, et al. Towards a paradigm shift in the treatment of chronic chagas disease. Vol. 58, Antimicrobial Agents and Chemotherapy. 2014. p. 635–9.

24. Calvet CM, Silva TA, Thomas D, Suzuki B, Hirata K, Siqueira-Neto JL, et al. Long term follow-up of trypanosoma cruzi infection and chagas disease manifestations in mice treated with benznidazole or posaconazole. PLoS Negl Trop Dis. 2020 Sep 1;14(9):1–14.

25. Castro JA, Montalto de Mecca M, Díaz Gómez MI, Castro GD. Enfermedad de Chagas: contribuciones del centro de investigaciones toxicológicas. Acta bioquímica clínica latinoamericana. 2014;49(1):73–82.

26. Galván IL, Pascual OM, Herrero-Martínez JM, Pérez-Ayala A, Hernández ML. Does progressive introduction of benznidazole reduce the chance of adverse events in the treatment of chagas disease? American Journal of Tropical Medicine and Hygiene. 2019;100(6):1477–81.

27. Molina I, Salvador F, Sánchez-Montalvá A, Treviño B, Serre N, Avilés AS, et al. Toxic profile of benznidazole in patients with chronic chagas disease: Risk factors and comparison of the product from two different manufacturers. Antimicrob Agents Chemother. 2015 Oct 1;59(10):6125–31.

28. Pinazo MJ, Muñoz J, Posada E, López-Chejade P, Gállego M, Ayala E, et al. Tolerance of benznidazole in treatment of Chagas' disease in adults. Antimicrob Agents Chemother. 2010 Nov;54(11):4896–9.

29. Pinazo MJ, Thomas MC, Bua J, Perrone A, Schijman AG, Viotti RJ, et al. Biological markers for evaluating therapeutic efficacy in Chagas disease, a systematic review. Vol. 12, Expert Review of Anti-Infective Therapy. Expert Reviews Ltd.; 2014. p. 479–96.

30. Navarro M, Norman FF, Pérez-Molina JA, López-Vélez R. Short report: Benznidazole shortage makes chagas disease a neglected tropical disease in developed countries: Data from Spain. American Journal of Tropical Medicine and Hygiene. 2012 Sep;87(3):489–90.

31. Molina-Morant D, Fernández ML, Bosch-Nicolau P, Sulleiro E, Bangher M, Salvador F, et al. Efficacy and safety assessment of different dosage of benznidazol for the treatment of Chagas disease in chronic phase in adults (MULTIBENZ study): Study protocol for a multicenter randomized Phase II non-inferiority clinical trial. Trials. 2020 Apr 15;21(1).

32. Muñoz-Calderón A, Santaniello A, Pereira A, Yannuzzi J, Díaz-Bello Z, Alarcón de Noya B. Susceptibilidad in vitro a Nifurtimox y Benznidazol de aislados de Trypanosoma cruzi obtenidos de pacientes venezolanos con enfermedad de Chagas infectados por mecanismos de transmisión oral y vectorial. Rev Ibero-Latinoam Parasitol. 2012;71(1).

33. Urbina JA. Specific chemotherapy of Chagas disease: Relevance, current limitations and new approaches. Acta Trop. 2010 Jul;115(1–2):55–68.

34. de Azevedo SLC, Catanho M, Guimarães ACR, Galvão TC. Genomic surveillance: a potential shortcut for effective Chagas disease management. Mem Inst Oswaldo Cruz. 2022;117.

35. Filardi LS, Brener Z. Susceptibility and natural resistance of Trypanosoma cruzi strains to drugs used clinically in Chagas disease. Vol. 81. 1987.

36. Silvestrini MMA, Alessio GD, Frias BED, Sales Júnior PA, Araújo MSS, Silvestrini CMA, et al. New insights into Trypanosoma cruzi genetic diversity, and its influence on parasite biology and clinical outcomes. Vol. 15, Frontiers in Immunology. Frontiers Media SA; 2024.

37. Campos MCO, Leon LL, Taylor MC, Kelly JM. Benznidazole-resistance in Trypanosoma cruzi: Evidence that distinct mechanisms can act in concert. Mol Biochem Parasitol. 2014;193(1):17–9.

38. Machado-Silva A, Cerqueira PG, Grazielle-Silva V, Gadelha FR, Peloso E de F, Teixeira SMR, et al. How Trypanosoma cruzi deals with oxidative stress: Antioxidant defence and DNA repair pathways. Vol. 767, Mutation Research - Reviews in Mutation Research. Elsevier B.V.; 2016. p. 8–22.

39. Jayawardhana S, Ward AI, Francisco AF, Lewis MD, Taylor MC, Kelly JM, et al. Benznidazole treatment leads to DNA damage in Trypanosoma cruzi and the persistence of rare widely dispersed non-replicative amastigotes in mice. PLoS Pathog. 2023 Nov 1;19(11 November).

40. Mejia AM, Hall BS, Taylor MC, Gómez-Palacio A, Wilkinson SR, Triana-Chávez O, et al. Benznidazole-resistance in trypanosoma cruzi is a readily acquired trait that can arise independently in a single population. Journal of Infectious Diseases. 2012 Jul 15;206(2):220–8.

41. Murta SMF, Lemos Santana PA, Jacques Dit Lapierre TJW, Penteado AB, El Hajje M, Navarro Vinha TC, et al. New drug discovery strategies for the treatment of benznidazole-resistance in Trypanosoma cruzi, the causative agent of Chagas

disease. Vol. 19, Expert Opinion on Drug Discovery. Taylor and Francis Ltd.; 2024. p. 741–53.

42. Lima DA, Gonçalves LO, Reis-Cunha JL, Guimarães PAS, Ruiz JC, Liarte DB, et al. Transcriptomic analysis of benznidazole-resistant and susceptible Trypanosoma cruzi populations. Parasit Vectors. 2023 Dec 1;16(1).

43. Zingales B, Macedo AM. Fifteen Years after the Definition of Trypanosoma cruzi DTUs: What Have We Learned? Vol. 13, Life. Multidisciplinary Digital Publishing Institute (MDPI); 2023.

44. Maya JD, Morello A. Inhibition of Glutathione Synthesis as a Potential Therapeutic Strategy Against Chagas' Disease. Journal of Biological Sciences. 2005 Oct 15;5(6):847–54.

45. Temperton NJ, Wilkinson SR, Meyer DJ, Kelly JM. Overexpression of superoxide dismutase in Trypanosoma cruzi results in increased sensitivity to the trypanocidal agents gentian violet and benznidazole. Vol. 96, Molecular and Biochemical Parasitology. 1998.

46. Bahia MT, De Figueiredo Diniz LDF, Mosqueira VCF. Therapeutical approaches under investigation for treatment of Chagas disease. Vol. 23, Expert Opinion on Investigational Drugs. Informa Healthcare; 2014. p. 1225–37.

47. Moraes CB, Giardini MA, Kim H, Franco CH, Araujo-Junior AM, Schenkman S, et al. Nitroheterocyclic compounds are more efficacious than CYP51 inhibitors against Trypanosoma cruzi: Implications for Chagas disease drug discovery and development. Sci Rep. 2014 Apr 16;4:1–11.

48. Sulleiro E, Muñoz-Calderon AqQ, Schijman AG. Role of nucleic acid amplification assays in monitoring treatment response in chagas disease: Usefulness in clinical trials. Vol. 199, Acta Tropica. Elsevier B.V.; 2019.

49. Cruz L, Vivas A, Montilla M, Hernández C, Flórez C, Parra E, et al. Comparative study of the biological properties of Trypanosoma cruzi I genotypes in a murine experimental model. Infection, Genetics and Evolution. 2015 Jan 1;29:110–7.

50. Sales PA, Molina I, Murta SMF, Sánchez-Montalvá A, Salvador F, Corrêa-Oliveira R, et al. Experimental and clinical treatment of Chagas disease: A review. Vol. 97, American Journal of Tropical Medicine and Hygiene. American Society of Tropical Medicine and Hygiene; 2017. p. 1289–303.

51. Kelly JM, Wilkinson SR. Mechanisms of resistance to antiparasitic drugs in Trypanosoma cruzi. Correlations between genotype and resistance. Rev Esp Salud Publica [Internet]. 2013;17–23. Available from: http://www.redalyc.org/articulo.oa?id=17027695003

52. Genois MM, Paquet ER, Laffitte MCN, Maity R, Rodrigue A, Ouellette M, et al. DNA Repair Pathways in Trypanosomatids: from DNA Repair to Drug Resistance. Microbiology and Molecular Biology Reviews. 2014 Mar;78(1):40–73.

53. Libisch MG, Rego N, Robello C. Transcriptional Studies on Trypanosoma cruzi – Host Cell Interactions: A Complex Puzzle of Variables. Vol. 11, Frontiers in Cellular and Infection Microbiology. Frontiers Media S.A.; 2021.

54. Vela A, Coral-Almeida M, Sereno D, Costales JA, Barnabé C, Brenière SF. In vitro susceptibility of trypanosoma cruzi discrete typing units (Dtus) to benznidazole: A systematic review and meta-analysis. PLoS Negl Trop Dis. 2021 Mar 1;15(3).

55. Andrade JM, Gonçalves LO, Liarte DB, Lima DA, Guimarães FG, de Melo Resende D, et al. Comparative transcriptomic analysis of antimony resistant and susceptible Leishmania infantum lines. Parasit Vectors. 2020 Dec 1;13(1).

56. Santi AMM, Murta SMF. Antioxidant defence system as a rational target for Chagas disease and Leishmaniasis chemotherapy. Mem Inst Oswaldo Cruz. 2022;117.

57. Cunha-Neto E, Allen PD, Stamatiou D, Benvenutti L, Higuchi ML, Koyama NS, et al. Cardiac Gene Expression Profiling Provides Evidence for Cytokinopathy as a Molecular Mechanism in Chagas' Disease Cardiomyopathy. Am J Pathol [Internet]. 2005;167(2):305–13. Available from: http://rana.lbl.gov/eisensoftware.htm

58. Reis-Cunha JL, Valdivia HO, Bartholomeu DC. Gene and Chromosomal Copy Number Variations as an Adaptive Mechanism Towards a Parasitic Lifestyle in Trypanosomatids. Curr Genomics. 2017 Sep 11;19(2).

59. Gupta I, Aggarwal S, Singh K, Yadav A, Khan S. Ubiquitin Proteasome pathway proteins as potential drug targets in parasite Trypanosoma cruzi. Sci Rep. 2018 Dec 1;8(1).

60. Lander N, Chiurillo MA. State-of-the-art CRISPR/Cas9 Technology for Genome Editing in Trypanosomatids. Vol. 66, Journal of Eukaryotic Microbiology. Blackwell Publishing Inc.; 2019. p. 981–91.

61. Mejía-Jaramillo AM, Ospina-Zapata H, Fernandez GJ, Triana-Chávez O. Transcriptomic analysis of benznidazole-resistant Trypanosoma cruzi clone reveals

nitroreductase I-independent resistance mechanisms. PLoS One. 2025 Feb 1;20(2 February).

62. García-Huertas P, Mejía-Jaramillo AM, González L, Triana-Chávez O. Transcriptome and Functional Genomics Reveal the Participation of Adenine Phosphoribosyltransferase in Trypanosoma cruzi Resistance to Benznidazole. J Cell Biochem. 2017 Jul 1;118(7):1936–45.

63. Coura JR, Borges-Pereira J. Chagas disease. What is known and what should be improved: a systemic review Doença de Chagas. O que é conhecido e o que deve ser melhorado: uma visão sistêmica. Vol. 45, Revista da Sociedade Brasileira de Medicina Tropical.

64. García-Huertas P, Mejía-Jaramillo AM, Machado CR, Guimarães AC, Triana-Chávez O. Prostaglandin F2α synthase in trypanosoma cruzi plays critical roles in oxidative stress and susceptibility to benznidazole. R Soc Open Sci. 2017 Sep 20;4(9).

65. Ariyanayagam MR, Fairlamb AH. Ovothiol and trypanothione as antioxidants in trypanosomatids [Internet]. Vol. 115, Molecular & Biochemical Parasitology. 2001. Available from: www.parasitology-online.com.

66. Couto N, Wood J, Barber J. The role of glutathione reductase and related enzymes on cellular redox homoeostasis network. Vol. 95, Free Radical Biology and Medicine. Elsevier Inc.; 2016. p. 27–42.

67. Santi AMM, Ribeiro JM, Reis-Cunha JL, Burle-Caldas G de A, Santos IFM, Silva PA, et al. Disruption of multiple copies of the Prostaglandin F2alpha synthase gene affects oxidative stress response and infectivity in Trypanosoma cruzi. PLoS Negl Trop Dis. 2022 Oct 19;16(10).

68. González L, García-Huertas P, Triana-Chávez O, García GA, Murta SMF, Mejía-Jaramillo AM. Aldo-keto reductase and alcohol dehydrogenase contribute to benznidazole natural resistance in Trypanosoma cruzi. Mol Microbiol. 2017 Dec 1;106(5):704–18.

69. Jamabo M, Bentley SJ, Macucule-Tinga P, Tembo P, Edkins AL, Boshoff A. In silico analysis of the HSP90 chaperone system from the African trypanosome, Trypanosoma brucei. Front Mol Biosci. 2022 Sep 23;9.

70. Mejía-Jaramillo AM, Fernández GJ, Palacio L, Triana-Chávez O. Gene expression study using real-time PCR identifies an NTR gene as a major marker of resistance to benznidazole in Trypanosoma cruzi. Parasit Vectors. 2011;4(1).

71. Douglas RL, Haltiwanger BM, Albisetti A, Wu H, Jeng RL, Mancuso J, et al. Trypanosomes have divergent kinesin-2 proteins that function differentially in flagellum biosynthesis and cell viability. J Cell Sci. 2020 Jul 9;133(13).

72. Docampo R, Moreno SNJ. The Role of Ca z+ the Process of Cell invasion by |ntracellular P_ras tes. Vol. 5, Aedes aegypti. Med. Vet. EntomoL.

73. Scarpelli PH, Pecenin MF, Garcia CRS. Intracellular ca2+ signaling in protozoan parasites: An overview with a focus on mitochondria. Vol. 22, International Journal of Molecular Sciences. MDPI AG; 2021. p. 1–12.

74. Márquez VE, Arias DG, Chiribao ML, Faral-Tello P, Robello C, Iglesias AA, et al. Redox metabolism in Trypanosoma cruzi. Biochemical characterization of dithiol glutaredoxin dependent cellular pathways. Biochimie. 2014;106:56–67.

75. Loureiro I, Faria J, Santarem N, Smith TK, Tavares J, Cordeiro-da-Silva A. Potential Drug Targets in the Pentose Phosphate Pathway of Trypanosomatids. Curr Med Chem. 2017 Dec 6;25(39):5239–65.

76. Hoyos Sanchez MC, Ospina Zapata HS, Suarez BD, Ospina C, Barbosa HJ, Carranza Martinez JC, et al. A phased genome assembly of a Colombian Trypanosoma cruzi TcI strain and the evolution of gene families. Sci Rep. 2024 Dec 1;14(1).

**SUPPLEMENTARY INFORMATION**

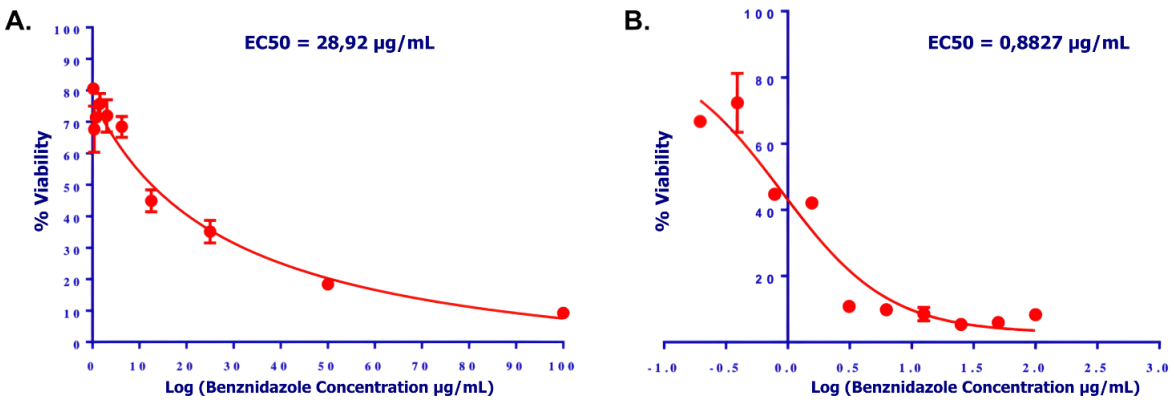


**Supplementary Figure 1.** Effect of Benznidazole on the Viability of a Resistant (**A**) and Susceptible (**B**) Strain of *T. cruzi*. This graph shows how Benznidazole concentration affects the viability of *T. cruzi* DA (**A**) and MG (**B**) strains. The EC50, indicating the concentration required to reduce viability to 50%, is marked on the descending curve.

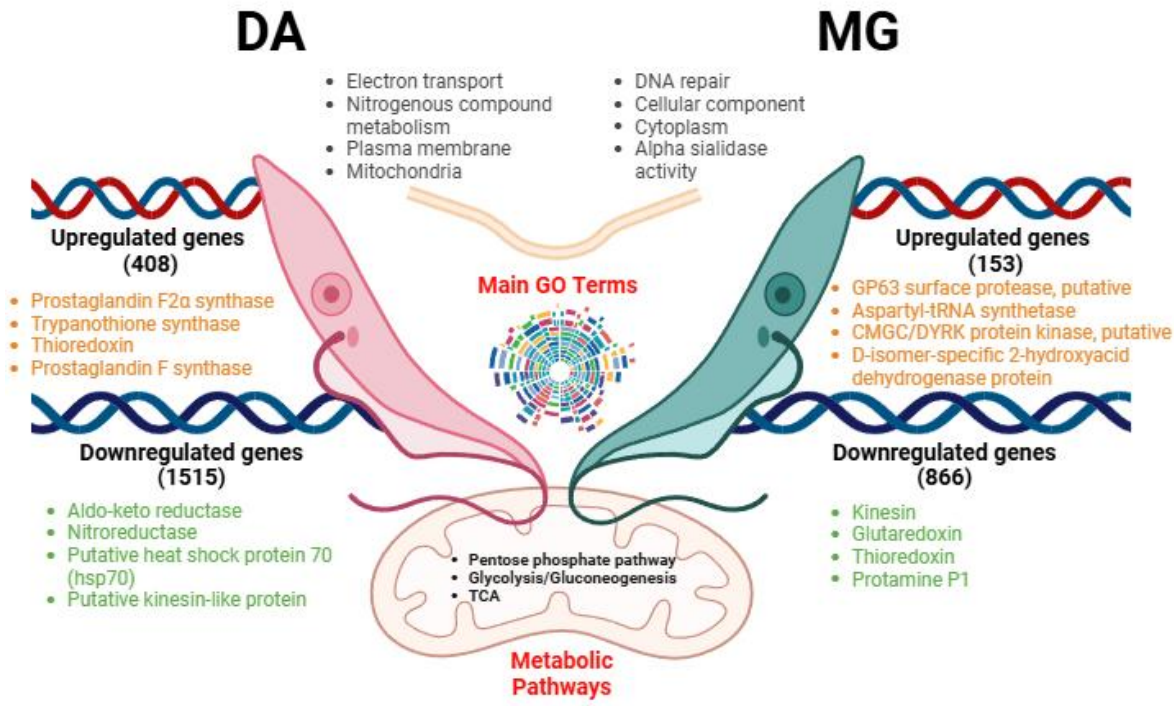


**Supplementary Figure 2.** Summary of the most relevant results of this study.

**Supplementary Table 1.** Top 50 Differentially Expressed Genes in the DA Strain: Genes with the Highest and Lowest Log2FoldChange.

| Gene_ID | log2FoldChange | lfcSE | padj | description |
|---|---|---|---|---|
| **UP REGULATED GENES** | | | | |
| TcBrA4_0042410 | 10,5710954 | 1,2189947 | 3,247E-17 | hypothetical protein |
| TcBrA4_0041370 | 8,435264495 | 1,2403938 | 4,709E-11 | hypothetical protein, conserved |
| TcBrA4_0038370 | 7,259559098 | 1,3048693 | 8,594E-08 | glutamamyl carboxypeptidase, pseudogene |
| TcBrA4_0072300 | 6,552823632 | 1,3936975 | 6,704E-06 | putative pteridine reductase 2 (ptr2) gene, pseudogene |
| TcBrA4_0076120 | 6,529788318 | 1,3638212 | 4,475E-06 | tubulin alpha-3 chain-like |
| TcBrA4_0044770 | 6,022827873 | 1,4349638 | 6,237E-05 | elongation factor 1-alpha (EF-1alpha) gene, pseudogene |
| TcBrA4_0187110 | 5,976314297 | 1,4689477 | 0,0001061 | dispersed gene family protein 1 (DGF-1, pseudogene), putative |
| TcBrA4_0062310 | 5,743753939 | 0,6601184 | 2,539E-17 | hypothetical protein |
| TcBrA4_0040580 | 5,666288304 | 0,9594501 | 1,243E-08 | hypothetical protein, pseudogene |
| TcBrA4_0013860 | 5,547217067 | 0,768354 | 2,644E-12 | CMGC/DYRK protein kinase, putative |
| TcBrA4_0007730 | 5,439699475 | 1,3851107 | 0,0001861 | SLACS reverse transcriptase |
| TcBrA4_0182210 | 5,420810677 | 0,9737846 | 8,443E-08 | surface protease GP63, putative |
| TcBrA4_0127210 | 5,385195048 | 0,8247845 | 2,76E-10 | E1-like ubiquitin-activating enzyme, putative |
| TcBrA4_0126640 | 5,209188821 | 0,8276605 | 1,205E-09 | elongation factor 1-alpha (EF-1alpha) gene, pseudogene |
| TcBrA4_0150160 | 5,046739005 | 1,4213152 | 0,0007606 | trans-sialidase, putative (fragment) |
| TcBrA4_0085420 | 5,040185749 | 0,6570137 | 9,805E-14 | hypothetical protein |
| TcBrA4_0117830 | 4,975555531 | 0,9803626 | 1,105E-06 | putative SLACS retrotransposable element |
| TcBrA4_0005210 | 4,927528161 | 1,1913602 | 8,027E-05 | hypothetical protein |
| TcBrA4_0131030 | 4,708744557 | 0,7467756 | 1,123E-09 | hypothetical protein, conserved |

| | | | | |
|---|---|---|---|---|
| TcBrA4_0117510 | 4,681063065 | 1,4710212 | 0,0026563 | hypothetical protein, conserved |
| TcBrA4_0120260 | 4,579134237 | 1,2850515 | 0,0007268 | hypothetical protein, pseudogene |
| TcBrA4_0153410 | 4,5777637 | 1,2536335 | 0,0005277 | trans-sialidase (pseudogene), putative |
| TcBrA4_0109730 | 4,48515515 | 0,3863152 | 5,969E-30 | hypothetical protein, conserved |
| TcBrA4_0149970 | 4,474844698 | 0,7734542 | 2,492E-08 | trans-sialidase, putative (fragment) |
| TcBrA4_0099360 | 4,417213721 | 0,4394365 | 9,964E-23 | PSP1-like protein, putative |
| TcBrA4_0131400 | 4,393372255 | 0,3965113 | 2,236E-27 | metacyclin III |
| TcBrA4_0185100 | 4,393105848 | 0,5623993 | 3,377E-14 | surface protease GP63 (pseudogene), putative |
| TcBrA4_0065030 | 4,379550628 | 0,716334 | 3,614E-09 | hypothetical protein, conserved |
| TcBrA4_0012180 | 4,364130819 | 0,195092 | 3,05E-108 | nuclear lim interactor-interacting factor, putative |
| TcBrA4_0074750 | 4,353826983 | 0,3176432 | 2,632E-41 | hypothetical protein |
| TcBrA4_0084790 | 4,247035704 | 0,2105777 | 3,137E-88 | hypothetical protein, conserved |
| TcBrA4_0122650 | 4,242477892 | 0,1944177 | 4,63E-103 | D-isomer specific 2-hydroxyacid dehydrogenase-protein, putative |
| TcBrA4_0108190 | 4,149491912 | 0,6730685 | 2,648E-09 | hypothetical protein, pseudogene |
| TcBrA4_0109630 | 4,143850931 | 0,4820463 | 6,157E-17 | hypothetical protein, conserved |
| TcBrA4_0086650 | 4,126228083 | 0,6850279 | 6,216E-09 | RNA-binding protein 4, putative |
| TcBrA4_0076800 | 4,093095097 | 0,830072 | 2,25E-06 | hypothetical protein |
| TcBrA4_0146480 | 4,058807918 | 0,9341926 | 3,334E-05 | trans-sialidase, putative |
| TcBrA4_0109720 | 4,055388774 | 0,7048906 | 2,987E-08 | hypothetical protein, conserved |
| TcBrA4_0126490 | 4,038316402 | 0,6331537 | 7,141E-10 | amino acid permease, putative |
| TcBrA4_0099450 | 4,017518021 | 0,1357488 | 5,91E-189 | hypothetical protein, conserved |

| | | | | |
|---|---|---|---|---|
| TcBrA4_00 49820 | 4,0014713 16 | 0,7002 188 | 3,719E -08 | putative glyceraldehyde 3-phosphate dehydrogenase, cytosolic |
| TcBrA4_01 66860 | 4,0006407 71 | 0,4216 813 | 2,255E -20 | mucin TcSMUGS, putative |
| TcBrA4_00 53480 | 3,9788693 32 | 0,7648 892 | 5,826E -07 | peptidylprolyl isomerase-like, pseudogene |
| TcBrA4_00 20880 | 3,9678328 66 | 0,8126 316 | 2,839E -06 | hypothetical protein, conserved |
| TcBrA4_01 02140 | 3,9279836 34 | 0,1100 241 | 5,21E- 275 | amino acid transporter |
| TcBrA4_01 67370 | 3,9206342 25 | 0,5133 922 | 1,272E -13 | mucin TcSMUGS, putative |
| TcBrA4_01 11150 | 3,8958657 27 | 0,8596 503 | 1,457E -05 | hypothetical protein |
| TcBrA4_01 22670 | 3,8444679 65 | 0,2760 154 | 1,298E -42 | hypothetical protein |
| TcBrA4_01 13060 | 3,8319729 17 | 0,7630 876 | 1,438E -06 | hypothetical protein, conserved |
| TcBrA4_00 48990 | 3,8221235 46 | 0,7717 46 | 2,026E -06 | hypothetical protein, conserved |
| **DOWN REGULATED GENES** | | | | |
| TcBrA4_01 23910 | - 5,2459725 96 | 0,4536 724 | 1,02E- 29 | hypothetical protein |
| TcBrA4_00 98950 | - 5,2669328 59 | 0,6825 621 | 6,981E -14 | KRI1-like family/KRI1-like family C-terminal, putative |
| TcBrA4_01 18930 | - 5,2680137 88 | 0,3503 628 | 1,816E -49 | hypothetical protein |
| TcBrA4_00 01320 | - 5,3037425 2 | 0,2580 602 | 1,48E- 91 | protein phosphatase inhibitor, putative |
| TcBrA4_01 26340 | - 5,3475986 25 | 1,4169 622 | 0,0003 353 | hypothetical protein |
| TcBrA4_00 25400 | - 5,3523765 17 | 0,1842 28 | 3,23E- 182 | hypothetical protein, conserved |
| TcBrA4_00 94480 | - 5,3766961 24 | 0,2572 268 | 1,142E -94 | Intraflagellar transport protein 74, putative |

| | | | | |
|---|---|---|---|---|
| TcBrA4_0159740 | -5,385793839 | 0,8102514 | 1,292E-10 | retrotransposon hot spot (RHS) protein, putative |
| TcBrA4_0163010 | -5,427835611 | 0,9753591 | 8,521E-08 | retrotransposon hot spot protein (RHS, pseudogene), putative |
| TcBrA4_0014910 | -5,467699743 | 0,2907141 | 7,451E-77 | hypothetical protein, conserved |
| TcBrA4_0022800 | -5,486814029 | 0,3561937 | 7,036E-52 | hypothetical protein, conserved |
| TcBrA4_0038710 | -5,543435006 | 0,3515379 | 2,506E-54 | kinesin K39 |
| TcBrA4_0030590 | -5,546801731 | 0,7694353 | 2,845E-12 | hypothetical protein, conserved |
| TcBrA4_0089340 | -5,57020729 | 0,6972556 | 8,585E-15 | hypothetical protein |
| TcBrA4_0133220 | -5,582041532 | 0,247057 | 2,26E-110 | hypothetical protein, conserved |
| TcBrA4_0019610 | -5,645183948 | 0,2226174 | 7,7E-139 | hypothetical protein, conserved |
| TcBrA4_0057530 | -5,659903215 | 0,28249 | 4,497E-87 | protein phosphatase 2C, putative |
| TcBrA4_0091780 | -5,678188794 | 0,210803 | 1,43E-156 | zinc finger protein 3 |
| TcBrA4_0161660 | -5,847284488 | 0,4497069 | 2,848E-37 | retrotransposon hot spot protein (RHS, pseudogene), putative |
| TcBrA4_0076510 | -5,921864302 | 0,7290499 | 2,985E-15 | trichohyalin, pseudogene |
| TcBrA4_0093080 | -5,978656902 | 0,1873852 | 1,02E-219 | hypothetical protein, conserved |

| | | | | |
|---|---|---|---|---|
| TcBrA4_0160880 | -6,051102187 | 0,9168675 | 1,754E-10 | retrotransposon hot spot protein (RHS, pseudogene), putative |
| TcBrA4_0073260 | -6,076420356 | 0,630907 | 5,86E-21 | Protein of unknown function (DUF1014), putative |
| TcBrA4_0159240 | -6,079370668 | 0,6298696 | 4,839E-21 | retrotransposon hot spot (RHS) protein, putative |
| TcBrA4_0063280 | -6,080327561 | 0,8487171 | 3,911E-12 | RNA-binding protein, putative |
| TcBrA4_0158860 | -6,282432985 | 1,4612288 | 4,055E-05 | retrotransposon hot spot (RHS) protein, putative |
| TcBrA4_0161610 | -6,31306772 | 1,1159258 | 5,129E-08 | retrotransposon hot spot protein (RHS, pseudogene), putative |
| TcBrA4_0041320 | -6,333021557 | 0,3927203 | 9,047E-57 | hypothetical protein, pseudogene |
| TcBrA4_0129560 | -6,394060296 | 0,2535244 | 2,17E-137 | 5'-AMP-activated protein kinase catalytic subunit alpha, putative |
| TcBrA4_0161650 | -6,460923427 | 0,5357135 | 3,183E-32 | retrotransposon hot spot protein (RHS, pseudogene), putative |
| TcBrA4_0096950 | -6,515180665 | 1,3210729 | 2,243E-06 | hypothetical protein, conserved |
| TcBrA4_0141720 | -6,522155275 | 1,2982739 | 1,424E-06 | trans-sialidase, Group VI, putative |
| TcBrA4_0042450 | -6,570050334 | 1,1014324 | 8,784E-09 | hypothetical protein, conserved |
| TcBrA4_0049070 | -6,677616387 | 0,3125623 | 7,91E-99 | small GTP-binding protein RAB6, putative |
| TcBrA4_0071830 | -6,890834648 | 1,3034664 | 3,751E-07 | NUP-1 protein, putative |

| | | | | |
|---|---|---|---|---|
| TcBrA4_0162970 | -6,913054551 | 1,2751314 | 1,847E-07 | retrotransposon hot spot protein (RHS, pseudogene), putative |
| TcBrA4_0054430 | -7,000990126 | 0,893361 | 2,776E-14 | ADP-ribosylation factor, putative |
| TcBrA4_0158410 | -7,069803096 | 0,8836086 | 7,787E-15 | retrotransposon hot spot (RHS) protein, putative |
| TcBrA4_0038590 | -7,225327978 | 1,3429603 | 2,299E-07 | putative kinesin-like protein |
| TcBrA4_0126360 | -7,643990181 | 1,3193589 | 2,375E-08 | hypothetical protein |
| TcBrA4_0000140 | -7,899963932 | 1,3567678 | 2,015E-08 | hypothetical protein, conserved |
| TcBrA4_0071780 | -7,979453861 | 1,2670375 | 1,177E-09 | hypothetical protein |
| TcBrA4_0006460 | -7,995426352 | 1,2909907 | 2,226E-09 | hypothetical protein, conserved |
| TcBrA4_0162980 | -8,212935785 | 1,2795134 | 5,544E-10 | retrotransposon hot spot protein (RHS, pseudogene), putative |
| TcBrA4_0096660 | -8,285276722 | 1,26842 | 2,714E-10 | hypothetical protein |
| TcBrA4_0048180 | -8,43919637 | 1,255792 | 8,005E-11 | hypothetical protein, conserved |
| TcBrA4_0135860 | -8,710207462 | 1,3307004 | 2,488E-10 | hypothetical protein |
| TcBrA4_0048590 | -9,477110682 | 1,2652795 | 3,768E-13 | protamine P1 |
| TcBrA4_0038700 | -9,980718938 | 1,2172184 | 1,618E-15 | hypothetical protein |

| | | | | |
|---|---|---|---|---|
| TcBrA4_01 35890 | -10,544157 39 | 1,2010 99 | 1,307E -17 | putative kinesin-like protein |

**Supplementary Table 2.** Top 50 Differentially Expressed Genes in the MG Strain: Genes with the Highest and Lowest Log2FoldChange.

| Gene_ID | log2FoldChange | lfcSE | padj | description |
|---|---|---|---|---|
| **UP REGULATED GENES** | | | | |
| TcBrA4_00 42410 | 11,572461 77 | 1,1894 3383 | 3,5047 E-21 | hypothetical protein |
| TcBrA4_01 09700 | 6,1745637 55 | 1,4032 3881 | 2,9081 E-05 | hypothetical protein, conserved |
| TcBrA4_01 83620 | 5,9738844 65 | 0,8982 586 | 1,5314 E-10 | surface protease GP63, putative |
| TcBrA4_00 46830 | 5,5613042 84 | 1,3645 1507 | 0,0001 1274 | aspartyl-tRNA synthetase |
| TcBrA4_00 13860 | 5,3720420 4 | 0,2636 3917 | 1,0285 E-89 | CMGC/DYRK protein kinase, putative |
| TcBrA4_01 22650 | 5,2926415 89 | 0,2036 6653 | 8,694E-146 | D-isomer specific 2-hydroxyacid dehydrogenase-protein, putative |
| TcBrA4_00 40580 | 5,2890273 14 | 0,8451 3311 | 1,8079 E-09 | hypothetical protein, pseudogene |
| TcBrA4_01 12700 | 5,2188355 38 | 0,7366 2334 | 8,54E-12 | hypothetical protein, pseudogene |
| TcBrA4_00 12180 | 4,9901530 6 | 0,1991 6969 | 1,631E-135 | nuclear lim interactor-interacting factor, putative |
| TcBrA4_01 09630 | 4,9032438 93 | 0,4214 1397 | 8,2142 E-30 | hypothetical protein, conserved |
| TcBrA4_00 65040 | 4,8198672 09 | 0,5407 0541 | 5,7652 E-18 | hypothetical protein, conserved |
| TcBrA4_01 09730 | 4,7735379 4 | 0,4918 1937 | 4,3799 E-21 | hypothetical protein, conserved |
| TcBrA4_01 08190 | 4,6863701 61 | 0,6489 2443 | 3,3141 E-12 | hypothetical protein, pseudogene |
| TcBrA4_00 99450 | 4,6841948 54 | 0,1331 9267 | 8,284E-267 | hypothetical protein, conserved |
| TcBrA4_01 09720 | 4,5175164 12 | 0,7304 6119 | 2,8231 E-09 | hypothetical protein, conserved |
| TcBrA4_00 70860 | 4,4616492 32 | 1,1991 9703 | 0,0004 4916 | hypothetical protein |

| | | | | |
|---|---|---|---|---|
| TcBrA4_00 57930 | 4,3655495 39 | 0,8758 759 | 1,9863 E-06 | hypothetical protein, conserved |
| TcBrA4_01 83610 | 4,3003367 41 | 0,3811 9131 | 4,2999 E-28 | surface protease GP63, putative |
| TcBrA4_01 81980 | 4,2282852 68 | 0,2597 4272 | 1,7395 E-57 | surface protease GP63, putative |
| TcBrA4_01 82440 | 4,2217547 5 | 0,4860 6619 | 4,0325 E-17 | surface protease GP63, putative |
| TcBrA4_00 84790 | 4,1972317 13 | 0,2317 0392 | 5,0694 E-71 | hypothetical protein, conserved |
| TcBrA4_00 65030 | 4,0233009 18 | 0,5665 1524 | 7,588E- 12 | hypothetical protein, conserved |
| TcBrA4_00 12710 | 3,9943674 14 | 0,6652 2278 | 8,2192 E-09 | hypothetical protein, conserved |
| TcBrA4_01 31030 | 3,9644135 29 | 0,2750 3736 | 2,9789 E-45 | hypothetical protein, conserved |
| TcBrA4_00 83500 | 3,7240529 2 | 0,1860 8745 | 1,4352 E-86 | hypothetical protein, conserved |
| TcBrA4_00 70340 | 3,7164298 18 | 0,2765 1629 | 1,8663 E-39 | hypothetical protein, conserved |
| TcBrA4_01 31400 | 3,6630577 97 | 0,3261 2221 | 7,3666 E-28 | metacyclin III |
| TcBrA4_01 66860 | 3,6553992 1 | 0,4750 0625 | 1,0696 E-13 | mucin TcSMUGS, putative |
| TcBrA4_00 74750 | 3,6446017 34 | 0,2802 2871 | 5,3184 E-37 | hypothetical protein |
| TcBrA4_01 02140 | 3,6353451 02 | 0,1121 7945 | 1,522E- 226 | amino acid transporter |
| TcBrA4_00 01310 | 3,5938560 43 | 0,1934 6776 | 1,1474 E-74 | Protein kinase domain, putative |
| TcBrA4_01 08650 | 3,5879972 34 | 0,6514 4471 | 1,3508 E-07 | hypothetical protein |
| TcBrA4_01 09660 | 3,5787131 12 | 0,9806 4915 | 0,0005 8373 | hypothetical protein, conserved |
| TcBrA4_01 51550 | 3,5708219 19 | 0,8062 9749 | 2,5654 E-05 | trans-sialidase (pseudogene), putative |
| TcBrA4_01 83600 | 3,5469506 21 | 0,3883 1249 | 8,4053 E-19 | surface protease GP63, putative |
| TcBrA4_01 82340 | 3,5282033 68 | 0,2770 7985 | 1,6636 E-35 | surface protease GP63, putative |
| TcBrA4_00 86650 | 3,5193706 31 | 0,2252 5347 | 4,9919 E-53 | RNA-binding protein 4, putative |

| | | | | |
|---|---|---|---|---|
| TcBrA4_00030350 | 3,441616237 | 1,68900539 | | tyrosine aminotransferase |
| TcBrA4_01010040 | 3,412923086 | 0,7500426 | 1,504E-05 | 60S ribosomal protein L40 |
| TcBrA4_01082060 | 3,411906106 | 0,22647579 | 2,3626E-49 | surface protease GP63, putative |
| TcBrA4_01082210 | 3,370457863 | 0,67695533 | 2,0387E-06 | surface protease GP63, putative |
| TcBrA4_00092310 | 3,328288068 | 0,16893227 | 6,4634E-84 | hypothetical protein, conserved |
| TcBrA4_01053410 | 3,26847753 | 0,96300863 | 0,0014277 | trans-sialidase (pseudogene), putative |
| TcBrA4_01000070 | 3,261672518 | 0,87860458 | 0,00046305 | hypothetical protein |
| TcBrA4_01052280 | 3,258491085 | 0,25300596 | 2,6942E-36 | trans-sialidase (pseudogene), putative |
| TcBrA4_01067370 | 3,248323324 | 0,37779189 | 8,284E-17 | mucin TcSMUGS, putative |
| TcBrA4_01051380 | 3,222530267 | 0,18755129 | 5,8233E-64 | trans-sialidase (pseudogene), putative |
| TcBrA4_00079760 | 3,202812253 | 0,99829745 | 0,00265094 | NAD(P)-dependent steroid dehydrogenase protein, putative (fragment) |
| TcBrA4_01026780 | 3,201371511 | 0,65816675 | 3,548E-06 | elongation factor 1-alpha (EF-1-alpha) |
| TcBrA4_01024780 | 3,188474541 | 0,19619239 | 2,6774E-57 | hypothetical protein, conserved |
| **DOWN REGULATED GENES** | | | | |
| TcBrA4_00000140 | -4,117988775 | 0,8483792 | 3,7207E-06 | hypothetical protein, conserved |
| TcBrA4_01012580 | -4,128085966 | 0,26797663 | 1,4361E-51 | hypothetical protein, conserved |
| TcBrA4_00009980 | -4,160910342 | 0,22227872 | 7,995E-76 | hypothetical protein, conserved |
| TcBrA4_00012120 | -4,214826986 | 0,1936282 | 2,386E-102 | Protein of unknown function (DUF2453), putative |
| TcBrA4_01052830 | -4,217068659 | 0,93938638 | 1,966E-05 | trans-sialidase (pseudogene), putative |

| | | | | |
|---|---|---|---|---|
| TcBrA4_00 49070 | -4,271893033 | 0,27994936 | 1,2794 E-50 | small GTP-binding protein RAB6, putative |
| TcBrA4_00 98510 | -4,297160722 | 0,19288316 | 3,403E-107 | proteasome activator protein pa26, putative |
| TcBrA4_01 62520 | -4,298131698 | 0,78272566 | 1,4754 E-07 | retrotransposon hot spot protein (RHS, pseudogene), putative |
| TcBrA4_01 15510 | -4,301088936 | 0,22537943 | 9,2515 E-79 | Mitochondrial outer membrane protein porin, putative |
| TcBrA4_01 61650 | -4,307962452 | 0,35394451 | 1,6187 E-32 | retrotransposon hot spot protein (RHS, pseudogene), putative |
| TcBrA4_00 26730 | -4,310214182 | 0,49643897 | 4,1415 E-17 | nucleosome assembly protein-like protein, putative |
| TcBrA4_00 99800 | -4,318520742 | 0,7874332 | 1,5324 E-07 | hypothetical protein, pseudogene |
| TcBrA4_01 61660 | -4,344453176 | 0,35344281 | 3,8027 E-33 | retrotransposon hot spot protein (RHS, pseudogene), putative |
| TcBrA4_00 82360 | -4,391774645 | 0,37530794 | 3,8669 E-30 | acylphosphatase, putative |
| TcBrA4_01 61640 | -4,408147455 | 0,59990407 | 1,3565 E-12 | retrotransposon hot spot protein (RHS, pseudogene), putative |
| TcBrA4_01 02730 | -4,460761527 | 0,30306589 | 3,7789 E-47 | hypothetical protein |
| TcBrA4_00 30590 | -4,463350176 | 0,16037141 | 6,206E-167 | hypothetical protein, conserved |
| TcBrA4_01 60880 | -4,475935254 | 0,30260759 | 1,3526 E-47 | retrotransposon hot spot protein (RHS, pseudogene), putative |
| TcBrA4_01 41540 | -4,576083699 | 1,20246558 | 0,0003 268 | trans-sialidase, Group V, putative |

| | | | | |
|---|---|---|---|---|
| TcBrA4_0054710 | -4,642050999 | 1,21100295 | 0,00029394 | UDP-Gal or UDP-GlcNAc-dependent glycosyltransferase, putative |
| TcBrA4_0001230 | -4,686698482 | 0,27343266 | 1,1573E-63 | hypothetical protein, conserved |
| TcBrA4_0141720 | -4,74629836 | 0,96348541 | 2,6317E-06 | trans-sialidase, Group VI, putative |
| TcBrA4_0159740 | -4,751796675 | 0,22913022 | 6,4742E-93 | retrotransposon hot spot (RHS) protein, putative |
| TcBrA4_0019610 | -4,805393931 | 0,17868176 | 5,76E-156 | hypothetical protein, conserved |
| TcBrA4_0063280 | -4,817874357 | 0,66942207 | 3,9301E-12 | RNA-binding protein, putative |
| TcBrA4_0097180 | -4,829651243 | 0,61032729 | 2,067E-14 | hypothetical protein, conserved |
| TcBrA4_0007900 | -4,834576053 | 1,21277135 | 0,0001612 | glutamamyl carboxypeptidase, pseudogene |
| TcBrA4_0082640 | -4,925941556 | 0,29248423 | 1,7579E-61 | putative mitochondrial RNA binding complex 1 subunit |
| TcBrA4_0163050 | -4,962126556 | 0,8385233 | 1,3616E-08 | retrotransposon hot spot protein (RHS, pseudogene), putative |
| TcBrA4_0158410 | -5,003022783 | 1,228181 | 0,00011368 | retrotransposon hot spot (RHS) protein, putative |
| TcBrA4_0087150 | -5,016511787 | 1,16831107 | 4,5809E-05 | cystathionine beta-synthase, pseudogene |
| TcBrA4_0007330 | -5,096545817 | 0,29727156 | 1,0893E-63 | proteasome 26S non-ATPase subunit 9, putative |
| TcBrA4_0057530 | -5,164599335 | 0,23451495 | 9,241E-105 | protein phosphatase 2C, putative |

| | | | | |
|---|---|---|---|---|
| TcBrA4_0135830 | -5,290964569 | 1,1466698 | 1,1276E-05 | hypothetical protein |
| TcBrA4_0091780 | -5,291967103 | 0,1668704 | 4,69E-217 | zinc finger protein 3 |
| TcBrA4_0158050 | -5,48684376 | 1,37412036 | 0,00015708 | retrotransposon hot spot protein (RHS), putative (fragment) |
| TcBrA4_0076090 | -5,567887342 | 2,04930092 | 0,01163696 | beta tubulin, pseudogene |
| TcBrA4_0163080 | -6,144923946 | 1,30104827 | 6,8606E-06 | retrotransposon hot spot protein (RHS, pseudogene), putative |
| TcBrA4_0073260 | -6,158782046 | 0,25176642 | 3,401E-129 | Protein of unknown function (DUF1014), putative |
| TcBrA4_0041320 | -6,292766792 | 0,3561462 | 1,3811E-67 | hypothetical protein, pseudogene |
| TcBrA4_0038690 | -6,756413447 | 1,33320932 | 1,3143E-06 | kinesin-like protein |
| TcBrA4_0022310 | -6,838781179 | 1,32248957 | 7,8046E-07 | hypothetical protein |
| TcBrA4_0092110 | -7,257172064 | 1,33511665 | 1,9876E-07 | hypothetical protein, pseudogene |
| TcBrA4_0162980 | -7,407570014 | 1,3044311 | 5,2891E-08 | retrotransposon hot spot protein (RHS, pseudogene), putative |
| TcBrA4_0048180 | -7,844164805 | 1,238657 | 1,1394E-09 | hypothetical protein, conserved |
| TcBrA4_0126360 | -7,956037691 | 1,25180182 | 9,8998E-10 | hypothetical protein |
| TcBrA4_0038700 | -9,186146754 | 1,22062104 | 3,7692E-13 | hypothetical protein |

| | | | | |
|---|---|---|---|---|
| TcBrA4_00 72800 | -9,204866248 | 1,63079064 | 6,3943 E-08 | (clone 5.9.1) alpha-tubulin, pseudogene |
| TcBrA4_01 35890 | -9,481397361 | 1,21481441 | 4,7013 E-14 | putative kinesin-like protein |
| TcBrA4_00 48590 | -9,939810673 | 1,71770971 | 2,8845 E-08 | protamine P1 |